European Journal of Nuclear Medicine and Molecular Imaging
https://doi.org/10.1007/s00259-024-07014-z

REVIEW ARTICLE

Systematic review: Mechanisms of photoactive nanocarriers for imaging and therapy including controlled drug delivery

Yapei Zhang[1,2] · Yunxiu Qiu[2,3] · Ali Bavandpour Karimi[2,4] · Bryan Ronain Smith[1,2,3,4]

Received: 2 July 2024 / Accepted: 2 December 2024
© The Author(s), under exclusive licence to Springer-Verlag GmbH Germany, part of Springer Nature 2024

Abstract

Background The design of smart, photoactivated nanomaterials for targeted drug delivery systems (DDS) has garnered significant research interest due in part to the ability of light to precisely control drug release in specific cells or tissues with high spatial and temporal resolution. The development of effective light-triggered DDS involves mechanisms including photocleavage, photoisomerization, photopolymerization, photosensitization, photothermal phenomena, and photorearrangement, which permit response to ultraviolet (UV), visible (Vis), and/or Near Infrared (NIR) light. This review explores recent advancements in light-responsive small molecules, polymers, and nanocarriers, detailing their underlying mechanisms and utility for drug delivery and/or imaging. Furthermore, it highlights key challenges and future perspectives in the development of light-triggered DDS, emphasizing the potential of these systems to revolutionize targeted therapies.

Method A systematic literature search was performed using Google Scholar as the primary database and information source. We searched the recently published literature (within 15 years) with the following keywords individually and in relevant combinations: light responsive, nanoparticle, drug release, mechanism, photothermal, photosensitization, photopolymerization, photocleavage, and photoisomerization.

Results We selected 117 scientific articles to assess the strength of evidence after screening titles and abstracts. We found that six mechanisms (photocleavage, photoisomerization, photopolymerization, photosensitization, photothermal phenomena, and photorearrangement) have primarily been used for light-triggered drug release and categorized our review accordingly. Azobenzene/spiropyran-based derivatives and o-nitrobenzyl/Coumarin derivatives are often used for photoisomerization and photocleavage-enabled drug delivery, while free radical polymerization and cationic polymerization comprise two main mechanisms of photopolymerization. One hundred two is the primary active radical oxygen species employed for photosensitization, which is a key factor that impacts the therapeutic effects in Photodynamic therapy, but not in photothermal therapy.

Conclusion The comprehensive review serves as a guiding compass for light-triggered DDS for biomedical applications. This rapidly advancing field is poised to generate breakthroughs for disease diagnosis and treatment.

Keywords Controlled drug release · Mechanism · Light responsive · Nanocarriers

Introduction

Nanotechnology has advanced significantly over the past few decades particularly in the field of nanomedicine. The encapsulation of drugs within nanoparticles (NPs) confers new advantageous properties upon them, such as enhanced bioavailability, improved pharmacokinetics/circulation, and reduced toxic side effects. The primary objectives of designing NPs as a delivery system include control over NP size and surface characteristics, as well as controllable release of loaded drug at an optimal therapeutic rate [1]. A variety of drug-loaded NPs have recently been developed, each with beneficial properties and limitations that must be properly

✉ Bryan Ronain Smith
smit2901@msu.edu

1 Department of Biomedical Engineering, Michigan State University, East Lansing, MI 48824, USA

2 Institute for Quantitative Health Science and Engineering, Michigan State University, East Lansing, MI 48824, USA

3 Department of Chemical Engineering and Material Science, Michigan State University, East Lansing, MI 48824, USA

4 Department of Cell and Molecular Biology, Michigan State University, East Lansing, MI 48824, USA

Published online: 26 December 2024

matched to the intended application; these include polymer NPs, liposomes, inorganic NPs, drug conjugates, hydrogel NPs, viral NPs, and metal-organic frameworks (MOFs), among others [2].

The outstanding innovations in the field of drug-loaded NPs notwithstanding, many drugs remain dangerous with high morbidity and even mortality without a carrier system that permits some form of targeted delivery specific to the disease site and/or to diseased cells. Targeted delivery takes many forms, from relatively simple antibody-drug conjugates and polymer-drug conjugates to precisely-engineered nanosystems and controlled release medical devices. Precision engineering of nanosystems can allow control over drug release including tuning rates of release. Indeed, controlled drug release is pivotal in modern disease treatment because it can significantly enhance the efficiency and safety of therapeutic regimens. Unlike traditional drug delivery methods, controlled release systems deliver drugs at a steady, predictable rate, allowing maintenance of drug levels within the therapeutic range over extended time periods [3]. This innovation minimizes the frequency of dosing, improving patient compliance, especially for chronic conditions that require long-term treatment. Additionally, controlled drug release minimizes the risk of side effects and toxicity by avoiding sudden systemic spikes in drug concentration. Therefore, controlled drug release is a crucial advancement in achieving better health outcomes for patients [4].

Controlled release strategies include intrinsic release (i.e., triggered by interaction with physiological molecules and environments *in vivo*) and extrinsically-triggered release. Extrinsic release strategies such as light, sound, and electromagnetism are appealing because they engineer control over drug release even after the materials have been injected in vivo, and they can be exquisitely targeted site-specifically simply by precisely aiming the energetic beam. To engineer these sorts of technologies into carriers, the burgeoning field of nanotechnology has paved the way for significant advances in medical therapeutics—particularly in the design of controlled drug delivery systems. Amongst these innovations, intrinsic stimuli including pH [5], redox [6], enzymes (matrix metalloproteinases, cathepsin, urokinase plasminogen activators) [7], Adenosine triphosphate (ATP) [8], and external physical stimuli (such as, temperature [9], electromagnetic fields [10], light [10], and sound [11]) as triggers to control drug release have drawn the most attention. Across the various stimuli, optical (light) energy is considered attractive for release of small molecules and other biomolecules from nanomaterials due to ease, cost, excellent spatiotemporal control, and precise control of optical parameters such as wavelength, irradiation density, and duration. Light commonly used for light-responsive delivery nanocarriers can be divided into three wavelength-based categories: ultraviolet (UV (200–400 nm), visible (Vis) (400–700 nm), and near-infrared (NIR) (NIR I: 700–1000 nm; NIR II: 1000-1700 nm) light [12, 13]. The energy range of UV light is appropriate to trigger cleavage, isomerization, rearrangement or cross-linking reactions in many photoactive chromophores. However, poor tissue penetration and high phototoxicity limit the application of UV light in clinical practice [14]. Compared to UV light, NIR and far-red Vis light (>600 nm) display higher tissue penetration depths due to endogenous chromophores' and biomolecules' (e.g., blood, water, and melanin) minimal attenuation and refraction. However, only relatively few photoresponsive chromophores respond directly to NIR because of the low energy of NIR light, which is insufficient to trigger most photoresponsive reaction processes including bond cleavage or isomerization [15]. As a result, two-photon excitation and NIR-to-UV upconversion have been developed to take advantage of the merits of NIR and UV/visible light for activating photoresponsive reactions. Two-photon excitation tends to be less damaging to tissue than one-photon excitation, as it employs photons with half the energy required for one-photon excitation, typically in the NIR region. This method reduces cell damage and improves tissue penetration by decreasing both photon absorption and scattering since lower energy can be used [16]. An advantage of two-photon methods is that it is label free—the cost is that a relatively high intensity of light must be used in order to ensure sufficient two-photon conversion events within a short timeframe in the focal plane. Compared with two-photon excitation, upconverting NPs (UCNPs), which produce NIR-to-UV upconversion, allow use of reduced intensity pulsed lasers. The 'price' for this low intensity approach, which is several orders of magnitude lower, is that UCNPs must be used/injected in order to produce the signal. Two-photon applications may require a standard fluorophore or certain types of biomolecular structures such as collagen to produce second-harmonics that can be imaged without fluorophores [17]. Moreover, the lower UC quantum yields and restricted irradiation wavelengths limit their applications [18].

Light-triggered drug release has potential uses across various clinical applications, including dermal, endoscopic, and intraoperative strategies. In dermal applications, drug-loaded NPs may be delivered to the disease site through subcutaneous, intravenous, or intratumoral injection, after which light is applied to the skin to trigger drug release at the site of application. This approach offers minimally-invasive treatment options. In endoscopic procedures, light-triggered drug delivery systems can be precisely activated within the body using light delivered via endoscopes equipped with light-emitting fibers [19]. Such methods allow local delivery of drugs through an image-guided approach in or near internal organs or tissues, providing a minimally-invasive alternative compared with traditional surgical methods. In addition, NIR-responsive nanocarriers have gained considerable

attention for use in image-guided surgery and intraoperative treatment. For example, FDA-approved intraoperative Fluobeam 800 imaging system [20] is valuable due to its ability to provide high-contrast signals in malignant tissue compared with the surrounding healthy tissue.

In this review, we systematically provide an overview on current advances in light-responsive nanodrug delivery systems and their mechanisms, including photocleavage, photoisomerization, photopolymerization, photosensitization, photothermal phenomena, and photorearrangement. We also cover current challenges and future perspectives on the development of light-responsive nanocarriers in practical controlled drug delivery and imaging applications.

Photoisomerization

UV-triggered photoisomerization

Isomerization is a reversible molecular conformational change between the *trans* conformation and the *cis* conformation. The "photo" prefix indicates that the change in conformation is caused by irradiation light generally in the UV, visible, or NIR part of the electromagnetic spectrum [11]. Photoisomerization is a crucial mechanism in controlled drug delivery due to its ability to trigger drug release with high spatial and temporal precision. Such precision allows non-invasive controlled drug release to be achieved using light as a stimulus. Also important is photoisomerization's compatibility with different nanocarriers (including liposomes, polymeric NPs, and mesoporous silica NPs) without significantly altering their physicochemical properties or stability. The more stable *trans* isomer has a planar, rod-like shape and low polarity, while the metastable *cis* isomer has a larger dipole moment with a bent or "banana-like" shape (Fig. 1a) [21, 22]. This alteration in spatial structure is accompanied by a change in polarity, which results in the destabilization of the isomer-modified nanocarriers and subsequent drug release. One way that photo-isomerization processes can be monitored is by ratiometric detection [23]. Gold NPs were modified with Azobenzene (AZO), and energy transfer was shown from the modified AZO to gold NPs (diameter <2 nm) upon 360 nm excitation, producing sensitized NIR emission (Fig 1b). The excitation efficiency of the gold core is much higher for the *trans* than the *cis* form of AZO, causing a 60% decrease in the NIR emission intensity from gold NPs due to the *trans-cis* photoisomerization. Thus, photoisomerization can be monitored by ratiometric detection of gold NP NIR emission upon dual UV (360 nm) and Vis (480 nm) excitation. This strategy might also be used to estimate drug release from NPs by monitoring the photoisomerization process in photoisomerization-enabled drug delivery systems.

Given their valuable optical properties, AZO and spiropyran (SP)-based derivatives are often used to engineer silica NPs, liposome, micelles and polymeric NPs for controlled drug release [24–26]. For example, Mesoporous Silica NPs (MSNs) have been used for photoisomerization-enabled drug delivery via application of photoisomerizable entities as molecular gatekeepers at the pore surface. Merocyanine (MC)/SP was grafted to MSN pores, and poly (amido amine) (PAMAM) dendrimers were linked to MSNs to serve as switchable gatekeepers via electrostatic interactions between negatively charged PAMAM and positively charged MC upon UV light irradiation (Fig 1c) [26]. Entrapped cargos with MSNs were released by opening the pores via MC transformation to the neutral SP form upon irradiation of visible light.

Zwitterionic UV-responsive polymeric micelles have also been used for drug delivery. For example, doxorubicin (DOX) loaded micelles were prepared with a notably low critical micelle concentration (CMC) value of 0.037 mg/mL by self-assembling SP-poly(2-methacryloyloxyethyl phosphorylcholine) polymer (SP-PMPC) [27]. Through reversible photochemical isomerization of hydrophobic SP to hydrophilic MC, the self-assembly and disassembly of SP-PMPC micelles can be precisely regulated by UV irradiation. Similar to the disassembly of UV-responsive micelles, monoacylated AZO amphiphile- ($AzoC10N^+$) based liposomes were used as a controlled drug delivery system by disrupting the liposomes via isomerization of $AzoC10N^+$ from its *trans* form to *cis* form (Fig 1d) [28]. Nonphospholipid liposomes were formed using decyl-azobenzyl-triethylammonium [$AzoC_{10}N^+$] and a sterol, cholesterol sulfate (Schol) (25/75 molar ratio). $AzoC_{10}N^+$ and Schol display similar lengths, maintaining liposomal stability. Sulforhodamine B (SRB) was encapsulated in and consistently released from liposomes for 2 mins upon excitation of 350 nm for 120 s and 150 s; thus, the *trans*−*cis* photoconversion remained even post-illumination and "static" leaky structures formed on liposomal membranes. Crucially, the *trans* form was swiftly restored by exposing the samples to 450 nm light for 180 s, as evidenced by the fact that no SRB was released following the illumination (Fig 1d).

In contrast to liposomes, polymersomes offer unique benefits such as enhanced structural durability, customizable architectural characteristics, and easy integration of multiple functionalities, such as encapsulation of NIR porphyrin dye for imaging, encapsulation of anti-cancer chemotherapeutic drugs, and modification of ligands on polymer chains to target molecules *in vitro* and *in vivo* [29]. Photochromic polymersomes with adjustable and reversible bilayer permeability were fabricated using poly(ethylene oxide)-b-PSPA (PEO-b-PSPA) diblock copolymers by exploiting the photoisomerization properties of SPA, a SP-based monomer (Fig 1e) [30]. SP moieties reversibly switched between a

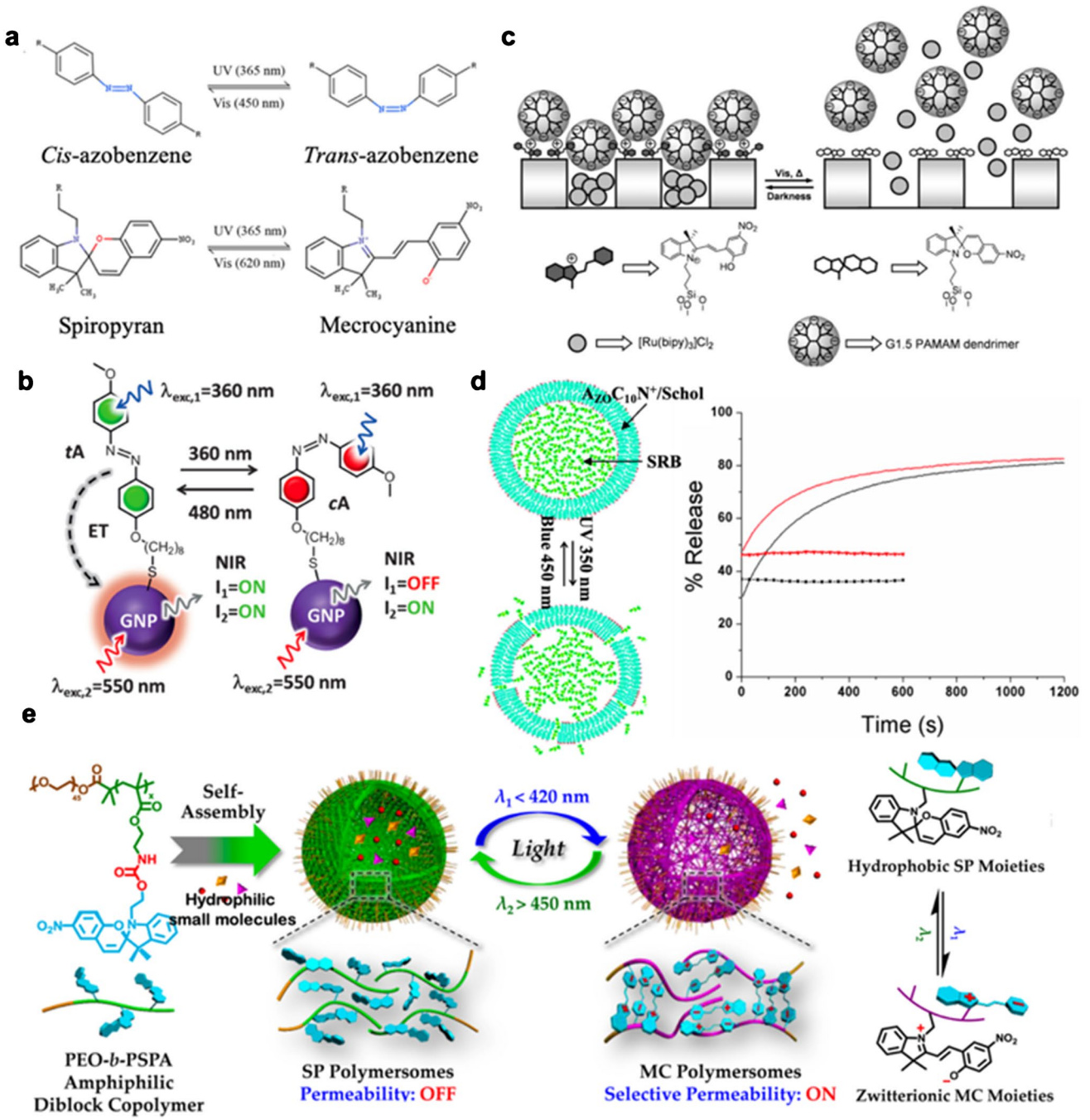


Fig. 1 a) Structural changes of AZO and SP upon UV light illumination [21]. Copyright 2021 Elsevier. b) Schematic of AZO modified gold NPs for producing sensitized NIR emission. ET: energy transfer. Copyright 2016 Angewandte Chemie. c) UV-triggered cargo release from MC/SP grafted MSNs by opening the pores through isomerization of MC/SP [26]. Copyright 2007 Wiley. d) UV-triggered disassembly of SP-based liposome and probe release upon 350 nm irradiation for 120 s (black line) and 150 s (red line) [28]. Copyright 2014 American Chemical Society. e) Amphiphilic PEO-b-PSPA diblock copolymers self-assemble into polymersomes. SP moieties within polymersome bilayers undergo reversible photo-triggered isomerization, resulting in membrane permeability switching from impermeable to selectively permeable and subsequent cargo release [30]. Copyright 2015 American Chemical Society

hydrophobic SP state (λ2 > 450 nm irradiation) and a zwitterionic MC state (λ1 < 420 nm irradiation), resulting in a shift from impermeable to selectively permeable. Interestingly, MC-based polymersomes sustained 5-dFu release upon short UV irradiation duration and on-demand release upon alternating UV−visible light irradiation due to the SP-to-MC transition. However, positively-charged doxorubicin hydrochloride (DOX·HCl, 580 Da) and negatively charged

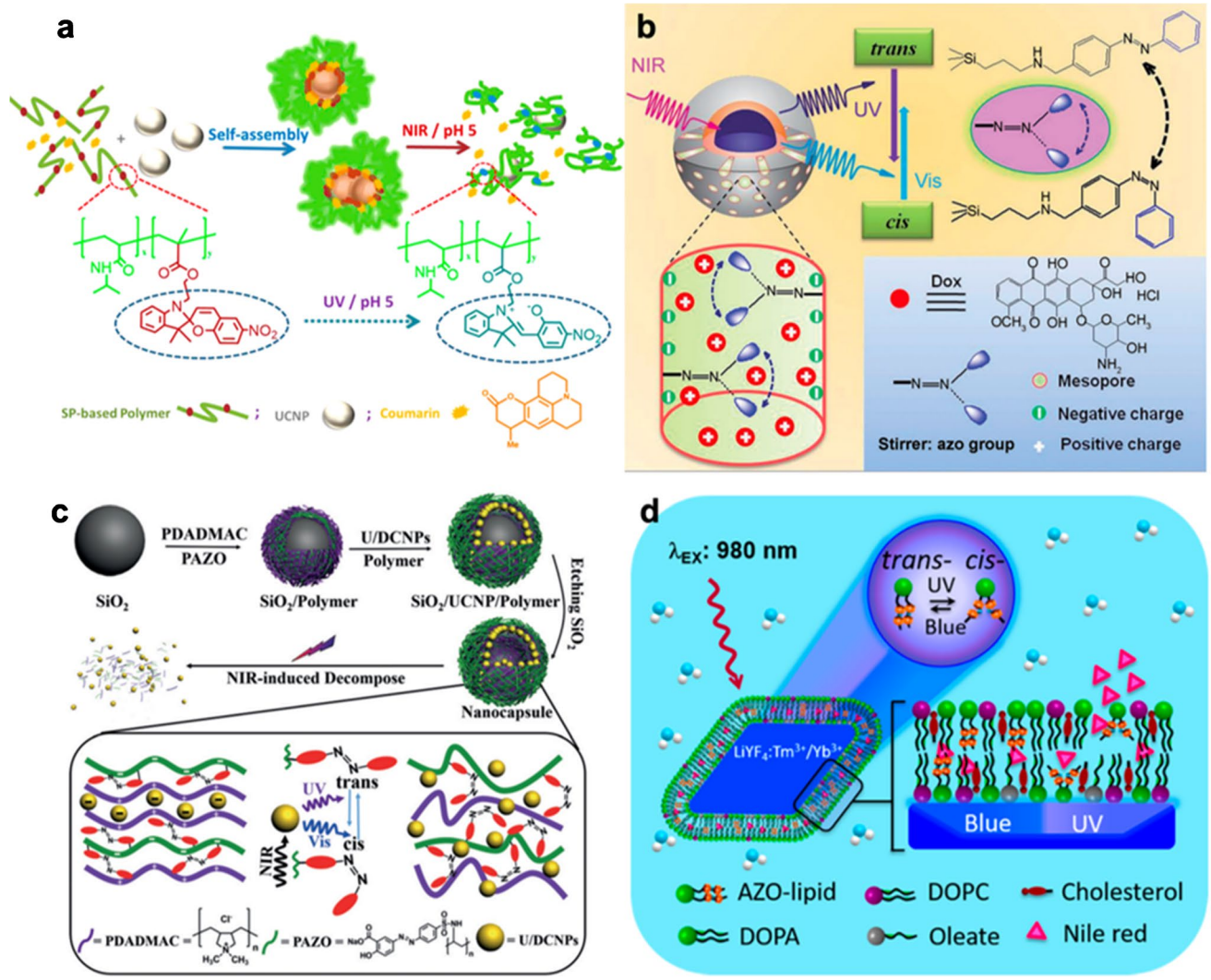


Fig. 2 Applications of NIR-triggered photoisomerization of SP and AZO in drug delivery. a) NIR triggered photoisomerization of SP to trigger the release of coumarin from micelles [31]. [32] [38] [37] Copyright 2016 American Chemical Society. b) 800 nm NIR-triggered Dox release through trans–cis photoisomerization of AZO molecules grafted in the mesopore network of a mesoporous silica layer on UCNPs. Copyright 2013 Wiley. c) Preparation of hollow polymer nanocapsules and NIR (800 nm)-induced decomposition in 180 nm nanocapsules, resulting in scattered polymer and 20 nm NPs. Copyright 2018 Wiley. d) Photoisomerization of AZO upon 980 nm NIR induced a volume change in the lipid layer and molecule release. 2018 American Chemical Society

calcein dye (623 Da) were not released from MC polymersomes, presumably due to their larger molecular size compared to 5-dFu (246 Da).

NIR-triggered photoisomerization

While UV light is photochemically valuable in diverse reactions, the phototoxicity, genotoxicity, and poor tissue penetration of this wavelength of light hamstring its biomedical utility. Thus, different mechanisms have been investigated to replace UV light with higher wavelengths such as NIR light to tune or convert photoisomerization toward a biologically friendly regime [22]. One strategy to apply NIR light for photoisomerization is to incorporate upconversion NPs (UCNPs) to combine lower energy (NIR) photons to produce a higher energy (UV) photon that can act on nearby isomerizable molecules. For example, copolymers incorporating SP, referred to as poly(isopropyl-acrylamide-co-SP methacrylate), were developed to self-assemble into micelles (Fig 2a) [31]. Within these micelles, the cores consisted of hydrophobic segments containing SP, while the shells consisted of hydrophilic segments containing poly(isopropylacrylamides). Concurrently, hydrophobic UCNPs and Coumarin 102 were encapsulated into the core alongside the self-assembly of the polymers. Under NIR irradiation, UCNPs emitted UV light, triggering isomerization

from the hydrophobic SP to hydrophilic MC. This transition disrupted the balance between hydrophilicity and hydrophobicity within the micelles, leading to controlled release of Coumarin 102. In another case, photoisomerization of AZO was used as a molecular "stirrer" to trigger DOX release from mesoporous silica-coated UCNPs upon NIR irradiation [32]. AZO was grafted into mesopores of the SiO_2 shell layer of UCNPs (Fig 2b). Upon NIR laser irradiation, the UCNPs emitted UV (350 nm) and visible (450 nm) light simultaneously, inducing continuous AZO rotation-inversion through the *trans*-to-*cis* photoisomerization of the AZO molecules within the mesopores. This continuous back and forth 'wagging' motion of AZO acted as a molecular impeller that triggered DOX release from the mesopores. While the utilization of UCNPs holds promise, this approach carries certain limitations for in vivo applications. Drawbacks include low quantum yield [33], a requirement for close proximity between UCNPs and AZO moieties due to the proximity-dependent nature of the energy transfer mechanism involved, the *in vivo* toxicity of UCNPs, and the fact that their clearance from the human body has not been comprehensively explored [34, 35].

Alternative methods to achieve drug release through the photoisomerization of AZO include micelle-triggered disassembly, nanocapsules decomposition, and increasing lipid bilayer volume upon NIR irridiation [24, 36, 37]. Trans-AZO and cyclodextrin (CD) exhibit robust affinities due to supramolecular host–guest interactions, whereas cis-AZO is not recognized by the CD cavity. Employing this chemical quirk, irradiation of NIR (800 nm) triggered the departure of AZO from the CD cavity, thereby causing disassembly of the AZO/CD-based hyperbranched conjugated polymer (HCP)–PEG micelles and thus DOX release [36]. To apply the nanocapsule decomposition approach, nanocapsules were prepared through a layer-by-layer assembly strategy of poly(diallyldimethylammonium chloride) and poly[1-{4-(3-carboxy-4-hydroxyphenylazo)benzenesulfonamido}-1,2-ethanediyl] (PDADMAC/PAZO) polymers on spherical SiO_2 colloids. These colloids were etched to create hollow-structure nanocapsules (Fig 2c) [38]. UCNPs and AZO were incorporated in the polymer shells during the polymer assembly process. Reversible photo-isomerization of AZO, stimulated by NIR (800 nm), induced continuous rotation–inversion movement, resulting in the decomposition of the 180 nm nanocapsules (initial size) into scattered polymers and 20 nm NPs. DOX was released from DOX-loaded nanocapsules during the decomposition to treat glioblastoma in a rodent model. 50% of loaded DOX was released in 60 mins upon NIR irradiation (1.5 W/cm^2).

Photoisomerization of AZO exhibits substantial utility in regulating lipid bilayer permeability [37]. AZO-modified lipid layers were used to coat UCNPs for molecular release (Fig 2d). Photoisomerization of AZO upon 980 nm NIR stimulation induced lipid bilayer disruption and volume change, initiating the release of Nile Red dye embedded within the hydrophobic core. While reversible photoisomerization strategies are promising for developing several diverse drug delivery platforms, some AZO molecules undergo irreversible degradation upon exposure to light or through enzymatic action by azoreductase, resulting in potential toxicity *in vivo* [39].

Photocleavage

ONB derivative-based photocleavage

Similar to photoisomerization, photocleavage allows non-invasive, spatiotemporally-precise triggering of drug release. The primary difference between photoisomerization and photocleavage is that while photoisomerization involves the rearrangement of atoms within a molecule, changing its geometric structure/conformation without breaking the molecule, photocleavage involves the cleavage of a chemical bond within a molecule upon exposure to light, which results in the creation of new molecules or reactive intermediates. In addition, photoisomerization is often reversible, allowing the same molecule to toggle between different forms under alternating light conditions. Photocleavage, on the other hand, typically results in irreversible bond breakage. Photocleavage has been used as an efficient albeit irreversible approach for constructing light-responsive photocleavable drug delivery systems based on reactions with photochromic copolymers. The C–O bond in the ester group of o-nitrobenzyl (ONB), C–C bonds in the cyclobutane ring of coumarin derivatives, and C-N bonds in 7-amino coumarin [40] are the most commonly-used photocleavable linkers [41]. These reactions, triggered by light exposure, lead to the rupture of one or more chemical bonds, which in turn can govern drug release through pre-designed structural modifications in the delivery systems. Photochromic molecules can be situated within the side chain, main chain, or middle block junction of copolymers, each imparting unique light-sensitive characteristics. Consequently, these three classes of photochromic copolymers produce the primary photocleavable modes of NP disruption and cargo release [12, 41].

One of the most extensively-researched photolabile groups, ONB derivatives find broad applications as part of organic syntheses and polymeric material production. Upon UV or NIR irradiation, ONB derivatives generate free radical intermediates, followed by hydrogen abstraction, resulting in the formation of resonance-stabilized benzylic radicals. Subsequent rearrangement of this radical species via a five-membered ring intermediate yields a liberated carboxylic acid along with a nitrosobenzaldehyde byproduct (Fig 3a) [11]. By taking advantage of ONB's photocleavage properties, an amphiphilic micelle based on block copolymer

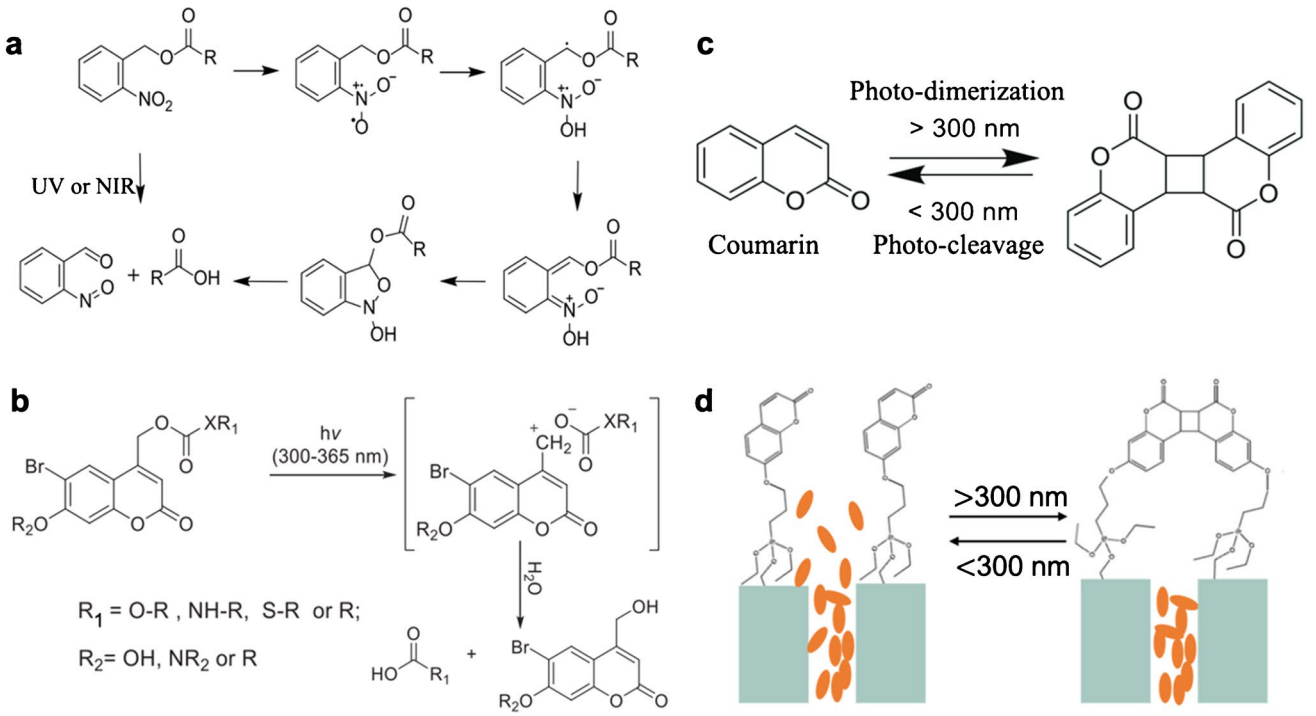


Fig. 3 Application of coumarin and ONB derivative photocleavage reactions in drug delivery. a) Mechanism of UV- or NIR-triggered photocleavage of ONB derivatives [11]. [12] [53] Copyright 2023 Springer. b) Photocleavage mechanism of a coumarin derivative. Copyright 2019 Wiley. c) Illustration of photo-dimerization (> 300 nm) and photo-cleavage (< 300 nm) reactions between two coumarin molecules. Copyright 2021 MDPI. d) Light-triggered drug release from coumarin-grafted MSNs. Figure was reproduced from Ref 50. Used with permission

N-succinyl-N'-4- (2-nitrobenzyloxy)-succinyl-chitosan (SNSC) was developed, including NIR dye in the core and 2-nitrobenzyl moieties on the hydrophobic block. SNSC was synthesized in three steps. First, chitosan was reacted with succinic anhydride to form N-succinyl-chitosan [42]. Next, the carboxyl group of 2-nitrobenzyloxy succinyl ester was activated using DCC/NHS. The activated ester was reacted with the free amine on N-succinyl-chitosan to form SNSC. Micelles based on SNSC were then formed through self-assembly under sonication. The micelles dissociate upon NIR illumination (765 nm). With a very long photocleavage reaction time of ~50 hrs, 100% of the fluorescein, which was used as a model drug, was released upon NIR irradiation [43].

The photocleavage properties of ONB have also been used to disrupt electrostatic equilibrium to release drug from NPs [44]. Positively-charged UV-labile poly(ethylene glycol) was synthesized with ONB as side groups, and then these polymers were grafted onto negatively charged silica-coated upconversion NPs (UCNP@silica) via electrostatic interaction. Upon NIR irradiation, UCNP@silica emitted UV light, initiating the ONB group cleavage and formation of carboxylic acid. This reaction intensified the electrostatic interaction between UCNP@silica and coated polymers, releasing the encapsulated drug [44]. In another application, ONB was utilized to modulate the hydrophobic/hydrophilic characteristics of polymers for drug release. A photolabile poly(4,5-dimethoxy-2-nitrobenzyl methacrylate) (PNBMA) shell was applied onto UCNP@silica. Upon NIR irradiation, PNBMA underwent photolysis, altering the surface properties of UCNP@silica@PNBMA from hydrophobic to hydrophilic. This transformation occurred as the hydrophobic ester group converted into a hydrophilic carboxylic acid. The size of UCNP@silica@PNBMA consequently increased from 108 nm to 140 nm, facilitating the release of DOX [45]. Another type of well-studied nanomaterial is gold NPs (Au NPs). In a simple scheme, an anticancer drug, 5-fluorouracil (5-FU), was attached to the surface of Au NPs by covalently conjugating the drug to ONB. Upon exposure to 365 nm UV irradiation, ONB underwent photocleavage, releasing the attached 5-FU to act on disease cells [46]. ONB has similarly been used to design photoresponsive liposomes, hydrogels, and mesoporous silica NPs [47]. However, despite its popularity, the cleavage of ONB results in the production of highly cytotoxic, reactive nitrosobenzaldehyde. This byproduct can strongly inhibit enzyme activity, potentially leading to undesired side effects *in vivo* [39]. Thus, ONB-driven photocleavage response is unlikely to be clinically translatable in most applications.

Coumarin derivatives-based photocleavage

The coumarin family encompasses numerous derivatives, known for their low toxicity, excellent stability, high molar absorption coefficients at longer wavelengths, and vibrant fluorescence emission characteristics [41]. Among the various coumarin derivatives, (coumarin-4-yl)methyl esters have garnered attention as one of the most rapidly reactive photosensitive groups. A single pulse of UV light at 337 nm for 0.5 ns can significantly weaken the C–O ester bond [21]. When subjected to UV or NIR light, the ester group undergoes decomposition into an ionic intermediate, subsequently leading to hydrolysis and the release of carboxyl and hydroxyl groups (Fig 3b). Coumarin-containing polymers have been widely used to prepare cross-linked micelles, polymeric NPs, hydrogels, dendrimers, and MSNs. For example, NIR-sensitive micelles were prepared using the block copolymer poly(ethylene oxide) (PEO) and poly(L-glutamic acid) bearing 6-bromo-7-hydroxycoumarin-4-yl-methyl groups, PEO_{114}-b-P(LGA-*co*-COU)$_{34}$ [48]. This micelle disassembled upon 794 nm NIR irradiation by removing coumarin groups from the polypeptide block, thereby destabilizing the micelles' hydrophilic–hydrophobic balance and resulting in the release of antibacterial and anticancer drugs. However, the photocleavage reaction time for coumarin-containing micelles is very slow; ~80% of the drug released after ~55 h NIR irradiation. Based on the same strategy, coumarin has also been used to design photocleavable 2-hydroxyethyl methacrylate-based NPs (> 350 nm UV light) [49], hydrogels (365 nm UV light) [40], and coumarin grafted MSNs [50]. For example, a low-molecular-weight hydrogel which exhibited photocleavage at the C-N bond (a new photosensitive site) in 7-amino coumarin upon UV irradiation (365 nm), was synthesized through π-π stacking interactions between gelators. Photocleavage-driven gel-sol transition triggered the release of the antineoplastic agent cytarabine hydrochloride from the hydrogel [40]. Unlike ONB-based compounds, coumarin derivatives exhibit reversible photo-dimerization and photo-cleavage properties (Fig. 3c), making them more adaptable for achieving temporally- and spatially-controlled drug delivery. For instance, 7-[(3-triethoxysilyl)propoxy] coumarin was grafted on the surface of MSNs, which had drug encapsulated in the pores. 365 nm UV light triggered the photo-dimerization of coumarin, resulting in pore closure. Conversely, 254 nm UV light triggered coumarin photocleavage, opening the pores and releasing drug (Fig. 3d) [50].

While coumarin and ONB have been extensively employed in the design of photosensitive drug delivery systems, NIR-wavelength photocleavage reaction times are much longer due to the low two-photon-absorptions of these chromophores than by UV light, exemplified by coumarin- or ONB-containing micelles. Furthermore, the simultaneous absorption of two photons necessitates high laser power density and the use of a femtosecond pulse laser is required [51] (less accessible and more resource-intensive compared to a UV lamp [52]). Therefore, incorporating a strategy such as UCNPs to augment light sensitivity and decrease irradiation duration is sometimes imperative to achieve efficient on-demand drug release. Moreover, research on coumarin-containing polymeric nanomedicines is relatively limited, likely owing to the intricate synthesis of photocleavable coumarin derivatives compared to commercially available ONB derivatives [41].

Photopolymerization

UV and visible light-triggered photopolymerization

As discussed in section "Photocleavage", photocleavage causes breakage of chemical bonds, often producing smaller molecular fragments. Conversely, photopolymerization leads to the generation of polymers from monomers. Photopolymerization is thus primarily used in the fabrication or assembly of nanomaterials such as drug-delivery nanocarriers. Photopolymerization processes occur via optical irradiation of monomers in the presence of a photoinitiator, which initiates a polymerization reaction by producing reactive species (cationic, anionic, free radicals). Photopolymerization can be performed with UV (330–450 nm), halogen lamp (400–520 nm), green LED (520-530 nm), or NIR light. Photopolymerization falls into two main categories as a function of variations in the reaction mechanism: free radical polymerization and cationic polymerization. Among these, free radical polymerization has broader application owing to the heightened reactivity of the free radicals it generates [54]. Propagation of the polymerization reaction is achieved by free radicals which attack suitable monomers with subsequent generation of free radicals involved in further propagation (Fig 4a) [11]. Propagation stops and polymerization terminates when the radical on the polymer chain encounters another radical [54]. Photopolymerization offers several advantages over conventional thermal and solution-based polymerization methods. First, it allows precise spatiotemporal control of the polymerization process by adjusting the exposure area and duration of light exposure. Second, it is a rapid process, often complete in just seconds to minutes. Third, photopolymerization can be implemented in water and organic solvents at room temperature. Last, photopolymerization can be employed to create or stiffen biomaterials *in situ*, offering a minimally invasive approach [55, 56] that can avoid some of the *in vivo* delivery problems associated with larger nanocarriers.

Photopolymerization has been widely used in hydrogel preparation. Hydrogels exhibit three-dimensional,

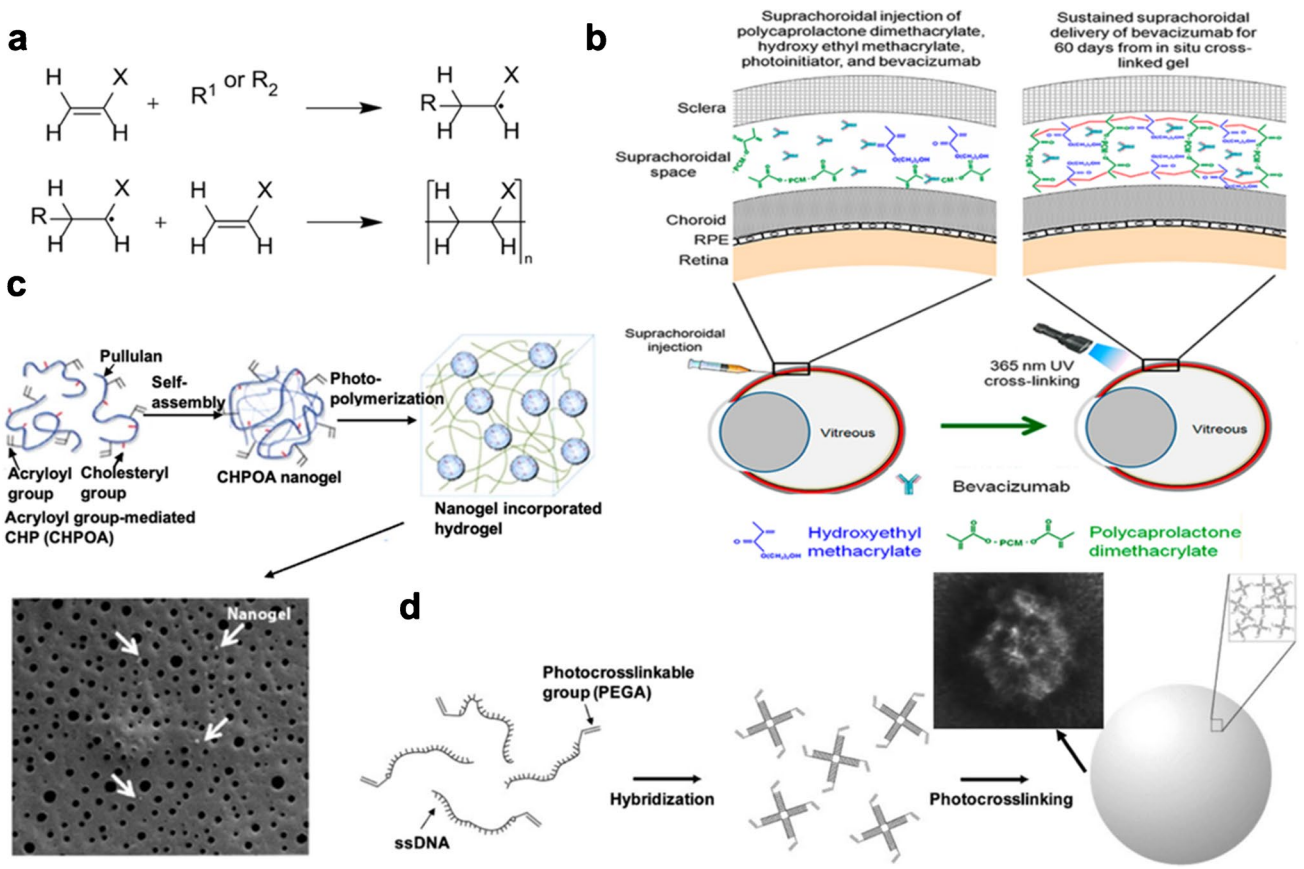


Fig. 4 Mechanism and application of UV/Vis light-triggered photopolymerization. a) Mechanism of photopolymerization reaction propagation [11]. [57] [58] [60] Copyright 2023 Springer. b) UV light-activated photopolymerization, in situ gel formation for sustained suprachoroidal delivery of bevacizumab. Copyright 2013 American Chemical Society. c) UV/Vis light activated nanogel-integrated hydrogels for controlled drug delivery. Copyright 2017 American Chemical Society. d) Preparation of DNA nanospheres by photopolymerizing X-DNA monomers upon UV illumination. Copyright 2010 Wiley

cross-linked polymeric structures, making them particularly appealing due to their substantial water retention and compatibility with biological systems. To facilitate sustained release of the drug bevacizumab in the suprachoroidal space, a light-activated gel composed of polycaprolactone dimethacrylate (PCM) and hydroxyethyl methacrylate (HEMA) was synthesized in situ within rat eyes. This process employed 2,2-dimethoxy-2-phenylacetophenone (DMPA) as a photoinitiator, exposed to 365 nm UV light for a duration ranging from 3 to 10 minutes (Fig 4b) [57]. The purpose was for drug release from the hydrogel to ameliorate choroidal neovascularization. Following 10 mins of UV irradiation, the gel/bevacizumab was confined at the injection site in excised rabbit eye suprachoroidal space, with sustained antibody release for approximately four months [57]. However, a potential flaw with the approach is that the free photoinitiator, decomposing into a benzoyl free radical, induced toxicity in ARPE (human retinal pigment epithelial cells) cells. This toxicity triggered oxidative stress and inflicted damage on lipids, proteins, and DNA within the eye.

Compared with plain hydrogels, nanogel-integrated hydrogels exhibit higher swelling behavior and drug loading amounts. For instance, poly(methacrylic acid-g-ethylene glycol) (P(MAA-g-EG)) and acryloyl group-modified cholesterol-bearing pullulan (CHPOA) served as a nanogel-integrated hydrogel. This hydrogel was developed by different photopolymerization approaches at visible (514 nm) and UV (300 nm) wavelengths to control delivery of the anticonvulsant drug, pregabalin (PGB) (Fig 4c) [58]. In this work, tetraethylene glycol dimethacrylate and erosin Y were chosen as the cross-linker and photoinitiator, respectively. Nanogels exhibited improved swelling ratios (~5% higher) compared to plain hydrogels, enhancing the PGB release percentage from 87.9% to 99.86%. In addition, nanogel-integrated hydrogels showed better morphological integrity when hydrogels were synthesized under visible light compared with those synthesized via UV light. Interestingly, photopolymerization has also been used to prepare contact lens material for ocular drug delivery using 2-hydroxy ethyl methacrylate (HEMA) and N-vinylpyrrolidone (NVP). This

approach applied poly ethylene glycol diacrylate (PEG-DA) as the cross-linker and initiator upon 15 mins of UV irradiation [59]. Subsequently, drug-loaded NPs (ranging from 52.3 to 83.4 nm) with PEG as the outer shell, poly HEMA as the inner shell, and polycaprolactone (PCL) as the hydrophobic core were incorporated into HEMA-co-VP hydrogel lenses. This method of NP incorporation into hydrogels offered prolonged drug release over 12 days. However, the hydrogel physicochemistry suffered, displaying an increased lens modulus and decreased ion and oxygen permeabilities. Such effects are potentially concerning for clinical translation because sufficient ion permeability is vital to reduc direct abrasion to the eye and a sufficient oxygen supply to the cornea helps maintain corneal integrity and provides defense against infection.

In addition to the application of photopolymerization to prepare hydrogels, UV light has also been used to polymerize DNA nanospheres. DNA can serve dual roles as both a genetic and a sort of generic material for molecular construction. Of particular interest is X-shaped DNA (X-DNA), which features four branched arms, as it offers multivalent functionalities capable of enabling simultaneous multiple crosslinking. Four acrylate-functionalized X-DNA monomers were synthesized by conjugating poly(ethylene glycol) acrylate groups (PEGA) to oligonucleotides. X-DNA monomers were subsequently photopolymerized to form monodisperse DNA nanospheres upon 10 min UV illumination to deliver DOX to mammalian cells (Fig 4d). The size of the DNA nanosphere (225 to 540 nm) is adjustable simply by varying the concentration of X-DNA monomers from 100 nM to 1 pM [60]. Intriguingly, DOX can exhibit dual functionality as an anticancer drug and as a co-catalyst for the polymerization of monomers such as acrylamide, acrylate, and methacrylates under blue light exposure [61]. By taking advantage of this property, polymeric NPs were prepared via photopolymerization of N,N-diethylacrylamide in the presence of poly(oligo(ethylene glycol) methyl ether acrylate) monomer and DOX upon irradiation of blue light (485 nm) [61]. Over 75% of DOX was released from the NPs into PBS within 7 days. Following uptake by murine melanoma (B16-F10) cells, DOX-loaded NPs effectively inhibited tumor cell proliferation by 40% after incubation for 24 hours. Although the precise mechanism of how DOX facilitates photopolymerization remains unclear, its ability to augment the polymerization process renders this strategy appealing for co-loading additional potentially synergistic drugs for combination therapy.

Green and NIR light-triggered photopolymerization

In addition to UV- and halogen lamp-triggered photopolymerization, green LED light has also been used to photopolymerize polymethyl methacrylate (PMMA)-based NPs [62]. In this process, photopolymerization took place under visible 520-530 nm irradiation, with Eosin Y/triethanolamine as photoinitiators and ethylene glycol dimethacrylate as the crosslinker. *In vitro* drug release (5-FU and MTX) studies demonstrated that the NPs exhibited a biphasic response with an initial burst release within 5 h, followed by a sustained logarithmic release for up to 32 h at pH 5 and pH 7 PBS. However, poor tissue penetration and high energy absorbance by tissues under 520-530 nm irradiation limit its application *in vivo*.

UV and visible light display limited penetration depth in organic materials such as biological tissues. Additionally, the use of high-energy irradiation, like UV light, can pose safety concerns and lead to undesirable reactions such as self-initiated polymerization, polymer degradation, and genotoxicity [54]. Therefore, for *in vivo* applications, NIR light is preferred for inducing polymerization due to its deeper penetration and reduced photodamage to biological systems. Thus, UCNP-assisted photopolymerization offers distinct advantages, including high chemical stability, low toxicity, resistance to photobleaching, narrow emission bandwidth, and significant anti-Stokes shifts [54, 63]. For instance, UCNP-assisted photopolymerization has been used to form a polymeric shell around UCNPs upon 980 nm NIR illumination, with 2-hydroxyethyl methacrylate (HEMA) as monomer and N,N'-ethylenebis- (acrylamide) (EbAM) as cross-linker, benzophenone/triethylamine as UV initiator and eosin Y/triethylamine as visible light initiator (Fig 5a) [63]. The polymer shell's properties can be tailored to be either hydrophilic or hydrophobic, charged or neutral, or chemically reactive or inert, depending on the monomers selected. The light intensity plays a crucial role in UCNP-assisted polymerization: higher laser intensity enhances curing depth and monomer conversion due to intensified upconversion emissions (Fig 5b) [64]. However, emission intensity reaches a plateau at a certain laser power level, and excessive laser power is likely to lead to overheating [54] and phototoxicity.

Photosensitization

Classification of ROS

Photosensitization is a critical component in photodynamic therapy (PDT), an increasingly valuable localizable therapeutic approach that applies light to promote eradication of disease states. Also known as photosensitization-induced oxidation, photosensitization is a process that generates radical oxygen species (ROS) such as singlet oxygen ($^1O_2$), hydroxyl radicals ($\bullet OH$), superoxide anions ($^{\bullet}O_2^-$) or

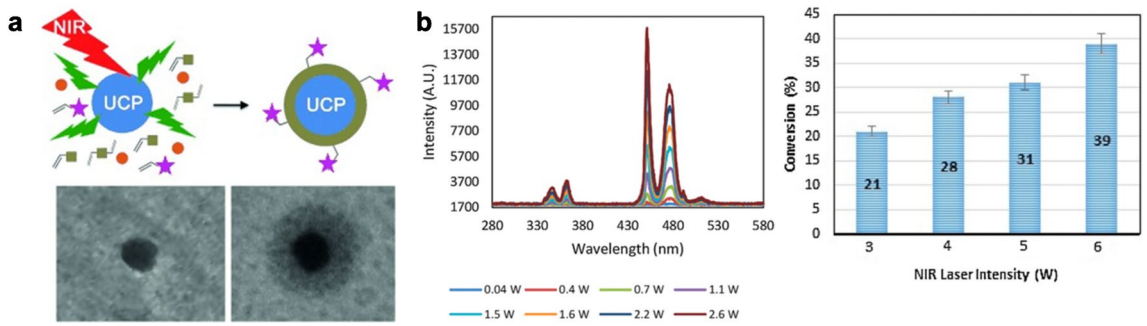


Fig. 5 Application of NIR light-triggered UCNP-assisted polymerization. a) Photopolymerized polymer shell on the surface of UCNPs upon NIR illumination [63]. [64] Copyright 2014 Wiley. b) Emission spectra of UCNPs under 980 nm NIR illumination and the monomer to polymer conversion efficiency under excitation across various laser intensities. Copyright 2016 Elsevier

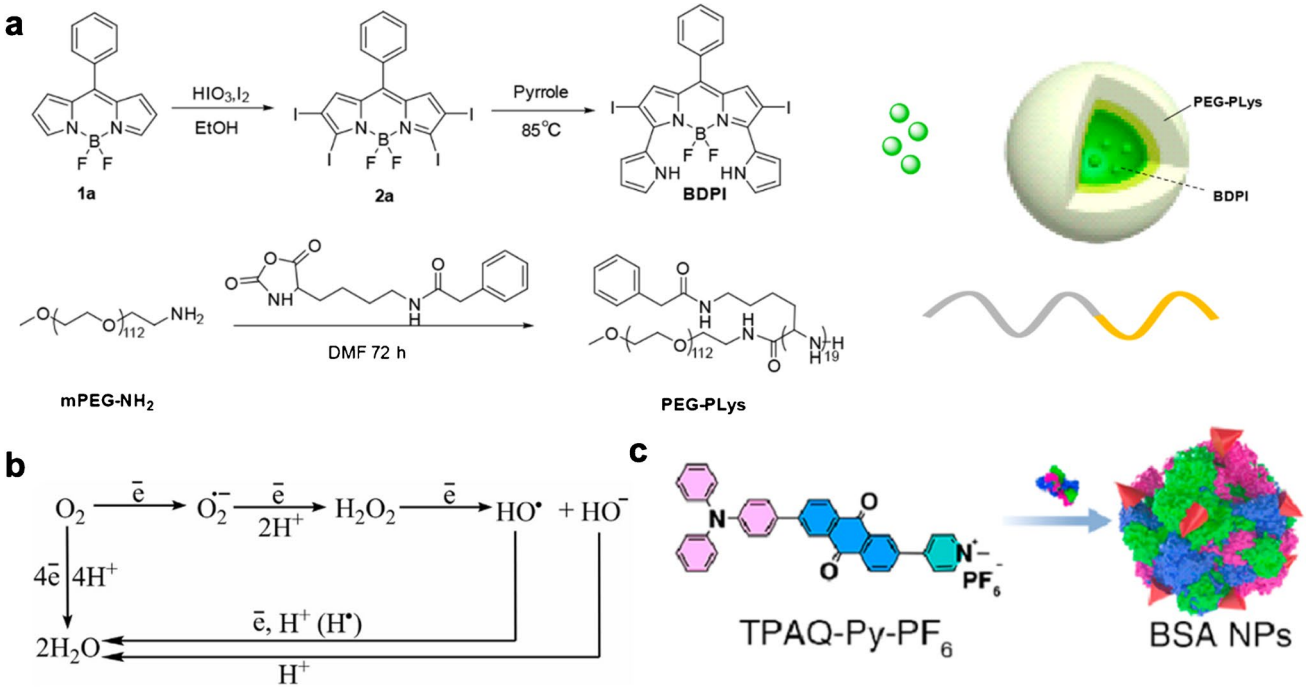


Fig. 6 a) Schematic of synthesis procedure of iodinated BODIPY loaded PEG−PLys NPs for PDT. Copyright 2018 American Chemical Society. b) Schematic of the formation processes for different ROS species. Copyright 2014 Elsevier. c) Preparation of TPAQ-Py-PF6-Albumin complex for PDT. Copyright 2023 American Chemical Society

hydrogen peroxide (H_2O_2) [21] to induce damage or death of target cells.

While $^1O_2$ is the primary active species in cancer PDT therapy, the $^1O_2$ quantum yield of most PSs (such as BODIPY) is low under low NIR power density, which restricts their PDT applications. To address this issue, a pyrrole-substituted iodinated BODIPY (BDPI) molecule was designed and encapsulated in mPEG5000-b-poly(ε-carbobenzoxy-L-lysine) (PEG−PLys) NPs for EMT6 tumor PDT treatment (Fig 6a) [65]. The $^1O_2$ quantum yield was 0.8 and some tumors disappeared without a wound upon low power illumination (660 nm, 25 mW/cm^2).

Mitochondria are the key organelles responsible for producing $^{\bullet}O_2^-$ through the one-electron reduction of the O_2 molecule. This $^{\bullet}O_2^-$ serves as the primary precursor for generating highly oxidizing or reducing species that trigger oxidative cascades within the cell [66]. Compared to $\bullet OH$, $^{\bullet}O_2^-$ reacts significantly less with non-radical species in aqueous solution [67]. The development of an organic NIR-II PS (TPEQM-DMA) allowed efficient production of $\bullet OH$ and $^{\bullet}O_2^-$ through a hypoxia (low O_2)-dependent (<0.1% O_2) type-I photochemical process under white light irradiation. TPEQM-DMA led to mitochondrial dysfunction and suppressed CT26 tumors growth after PDT treatment (100 mW/cm^2, 10 mins) [68].

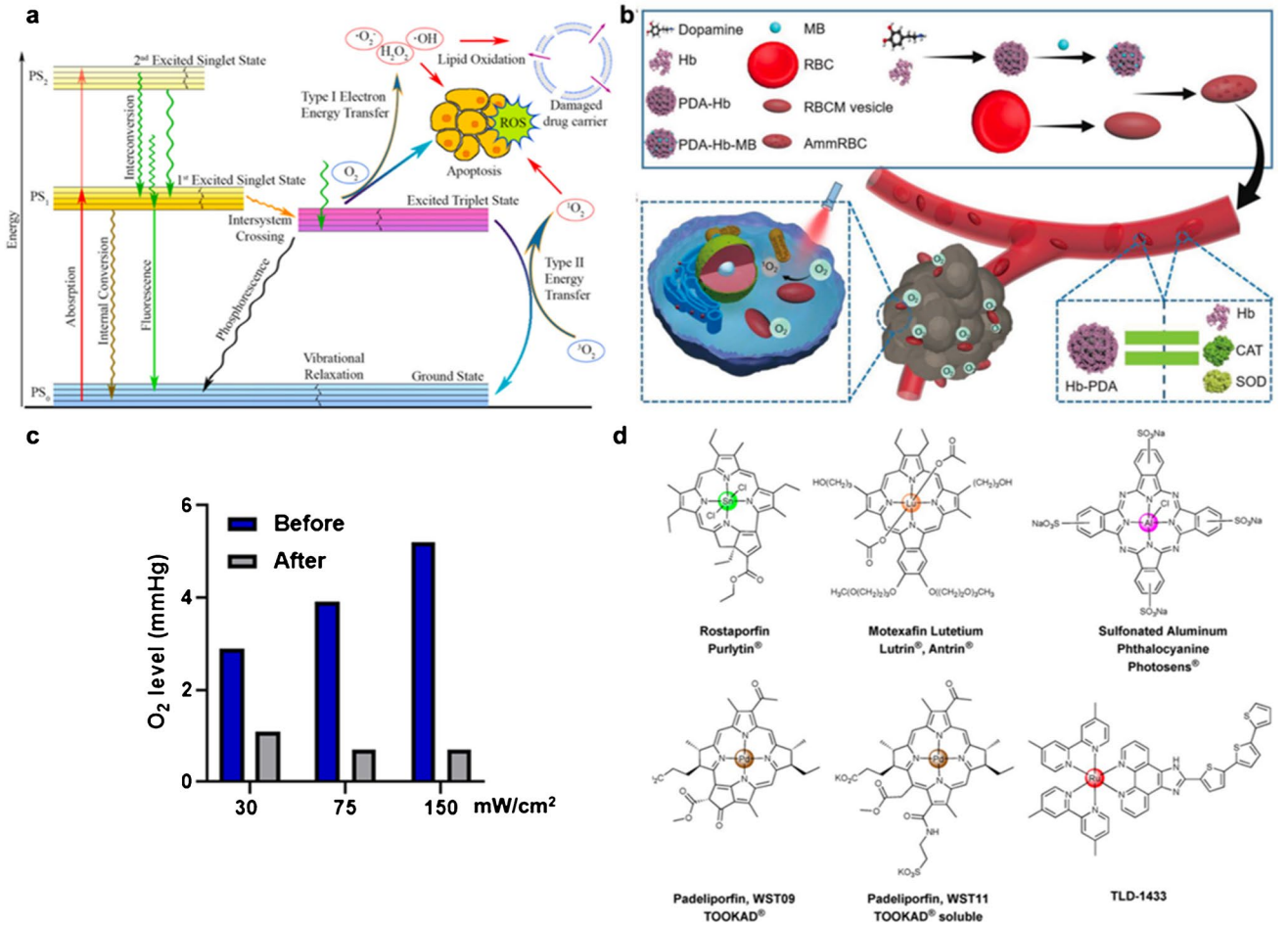


Fig. 7 Mechanism and applications of photosensitization. a) The process of photosensitization-induced oxidation upon light illumination [21]. [74] [77]. Copyright 2021 Elsevier. b) Preparation of AmmRBC to boost the $^1O_2$ generation for enhanced PDT. Copyright 2018 Wiley. c) Effect of light illumination on O_2 levels in murine RIF tumor. Data were adapted from Ref 70. Used with permission. d) Structure of metal complex PSs in clinical trials. Copyright 2021 Wiley

Singlet oxygen is not the only key cytotoxic ROS in PDT. H_2O_2 is produced through the dismutation reaction of $^{\bullet}O_2^-$. After accepting one electron, H_2O_2 can break down into $\bullet OH$ and OH^-. Subsequently, the $\bullet OH$ can interact with an electron and a proton, leading to the formation of H_2O (Fig 6b) [69]. Primarily generated through the Fenton reaction involving H_2O_2 and metal species, such as iron or copper, $\bullet HO$ is the most reactive radical [68]. $\bullet HO$, with its strong oxidizing ability, is considered the primary antitumor agent in type I PDT [70]. Leveraging this characteristic, a cationic photosensitizer (PS), TPAQ-Py-PF6 (TPA=triphenylamine, Q=anthraquinone, Py=pyridine), was developed and incorporated into the hydrophobic domain of bovine serum albumin NPs (BSA NPs) (Fig 6c). The electron-rich microenvironment of BSA facilitated $\bullet HO$ generation, resulting in a strong antitumor PDT effect upon white light irradiation (80 mW/cm^2, 10 mins) [70].

Factors that affect PDT efficiency

PDT requires the presence of molecular oxygen, a PS, and excitation light in the absorption regime of the photosensitizer (generally in the red spectral region, $\lambda \geq 600$ nm). Upon light absorption, a PS undergoes transformation from its ground state (PS_0) to a short-lived (a few nanoseconds or less) intermediate electronically-excited and unstable singlet state (PS_1). Subsequently, the PS_1 state can either i) decay back to the PS_0 state by losing energy via fluorescence emission or heat production; or ii) progress to a more stable, less energetic and long-lived (up to tens of μs) electronically-excited state (PS_2) through spin conversion of the electron in the higher-energy orbital (Fig 7a) [21, 71].

Many factors affect PDT efficiency. For example, $^1O_2$ is the predominant cytotoxic ROS produced during PDT [72]. Yet the short lifetime of $^1O_2$ (<0.04 μs) restricts the

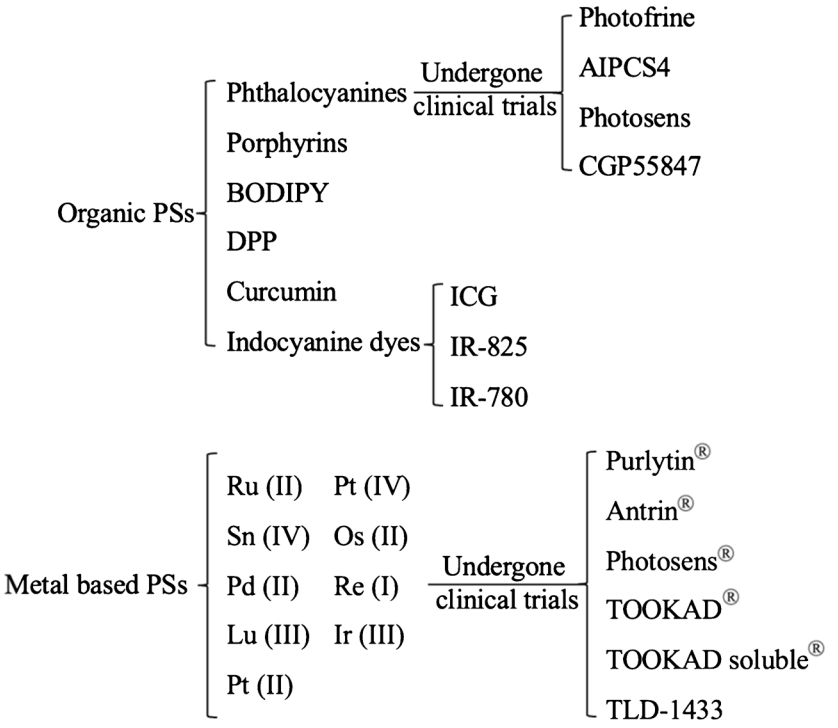


Fig. 8 Schematic diagrams of organic and metal-based photosensitizers

oxidative damage induced by PDT affecting such a molecule to a spherical volume of ~20 nm radius, centered at its production point [73]. Other factors that affect PDT include the local oxygen level, oxygen consumption rate, and the type of light applied (e.g., continuous or pulsed laser). Tumor tissue often presents distinct pathological characteristics such as severe hypoxia, which limits PDT effectiveness. To overcome this limitation, a complex of hemoglobin, polydopamine, and photosensitizer was encapsulated into artificial red blood cells (AmmRBC), which showed 10-fold higher corpuscular hemoglobin than natural RBCs (Fig 7b) [74]. Continuous wave (CW) light at high fluence rates caused significant oxygen depletion and reduction of PDT effects. For example, the O_2 level in murine radiation-induced fibrosarcoma (RIF) tumor decreased from 2.9~5.2 mmHg (averaged in 10 mice) to 0.7~1.1 mmHg after 1 min light illumination (630 nm, 30~150 mW/cm^2, 5mg/kg Photofrin photosensitizer) [75] (Fig 7c). However, O_2 levels rebounded to normal once illumination is interrupted. In addition, mice treated with PDT at 30 mW/cm^2 fluence show enhanced tumor inhibition compared with 150 mW/cm^2[75]. PDT's cytotoxic effects on mouse renal carcinoma cells (Renca) using pulsed light was significantly lower than that using CW light [76]. Therefore, PDT optimization requires careful consideration of factors such as oxygen level and consumption as well as the type of light used in order to enhance therapeutic efficacy, particularly in the context of tumor-specific characteristics such as hypoxia.

Another key factor that affects photosensitization is the class of photosensitizer. Commonly used organic PSs include porphyrins, phthalocyanines, indocyanine dyes, BODIPYs, DPP, and curcumin (Fig 8). Porphyrins exhibit hydrophobic properties, and their absorption bands (400~600 nm) fall within the visible range, limiting their utility in PDT applications [78]. Phthalocyanines exhibit absorption in the 650 ~ 800 nm range with high singlet oxygen-producing ability [79]. Phthalocyanines are also capable of forming metal complexes with Zn, Al, and Si atoms et al., which further increase their singlet oxygen-producing ability. Several phthalocyanine-based photosensitizers have undergone clinical trials. For instance, photofrine is approved for cancer treatment [77], Aluminum(III) chloride phthalocyanine tetrasulfonate (AlPCS4) is approved for PDT of superficial bladder cancer [78], and Photosens received clinical approval in Russia to treat skin, breast, gastrointestinal, lung malignancies, and eye neovascularization [80]. While CGP55847, a liposomal formulation of unsubstituted ZnPc developed by Ciba-Geigy, entered Phase I/II clinical trials on squamous cell carcinomas of the upper aerodigestive tract, no human clinical trial data is yet available [79]. Indocyanine dyes, including clinically-used indocyanine green (ICG), IR-825, and IR-780, have been used for fluorescence imaging and PDT due to their NIR absorption and excellent biocompatibility. While the introduction of heavy atoms to indocyanine dyes can improve $^1O_2$ generation, cytotoxicity is simultaneously increased [78]. Additionally, indocyanine dyes exhibit

low photostability and high levels of photobleaching [81]. A potential limitation is that most organic PSs tend to exhibit aggregation-induced fluorescence quenching and reduced ROS generation. This effect is particularly pronounced when PSs are encapsulated within NPs, leading to diminished PDT effects.

Beside the traditional organic PSs, metal-containing polypyridine or tetrapyrrolic atoms (for example, Ru (II), Sn (IV), Pd (II), Lu (III), Pt (II), Pt (IV), Os (II), Re (I), or Ir (III)) are being intensely investigated as PSs. All PSs mentioned in this section are summarized in Fig. 8. Ru (II)-based PSs usually display high water solubility, high $^1O_2$ production rate, high photochemical stability, prolonged excited state lifetime, and little or no photobleaching [77, 78, 82]. However, Ru (II)-based PSs lack significant absorption in the primary biological optical window (600−900 nm) and generally display poor tissue penetration depth [82]. Similarly, Ir (III)-based PSs exhibit high $^1O_2$ production capability due to their longer excited lifetime (up to ~2 μs) [83]. In addition, the photochemical and photophysical properties of Ir(III)-based PSs advantageously can be easily tuned by their ligands through introduction of electron-withdrawing and electron-donating groups [78]. However, i) poor water solubility and cytotoxicity of Ir(III)-based PSs hinders their application, ii) the inherently short excitation wavelength results in poor tissue penetration, a key obstacle in clinical application, and iii) their PDT efficacy is directly related to tumor oxygen content [84]. Nonetheless, important progress has been made with Ir(III) complexes in PDT. For instance, Ir(III) polypyridine poly(ethylene glycol) (PEG) complexes were designed to increase Ir(III) biocompatibility [85], Ir (III) based MOFs were developed for deep PDT application upon X-ray irradiation [86], and oxygen-independent Ir (III) anthraquinone complex as a mitochondrion-localized carbon-radical initiator could damage the mitochondrial membrane upon irradiation [87]. Similar to Ir (III)-based PSs, Re (I)-based PSs do not show good solubility in aqueous media, but they advantageously display lower heavy-metal toxicity compared with other metal-based PSs [88]. Os-based PSs show distinct advantages over other transition metal compounds, including those containing Ru, Ir, and Pt complexes. These compounds absorb light at longer wavelengths and exhibit emission maxima in the near-infrared region, enhancing deep tissue penetration [89].

Several of these metal complexes are undergoing clinical trials (Fig 7d) [77]. For example, Ru (II)-based PSs (TLD-1433) has entered into phase II clinical trials in Canada for bladder cancer, and padeliporfin/WST09 (TOOKAD), a palladium-coordinated bacteriochlorophyll α, is in phase I/II clinical trials to treat prostate cancer [77]. Nonetheless, most PSs operate via the O_2-dependent Type-II PDT mechanism through energy transfer between excited PSs and adjacent tumor-endogenous O_2 to yield toxic singlet oxygen ($^1O_2$). Because of this mechanism, the lack of oxygen in aggressive and drug-resistant tumors poses a significant challenge for PDT treatment. To avoid this problem, alternative approaches have been developed, such as the photoactivation of Pt-based PSs display O_2-independent manner [89, 90]. Furthermore, although photosensitizers induce cytotoxicity only upon light exposure, they also tend to accumulate in tumor surroundings due to nonspecific cellular uptake, potentially leading to damage to surrounding healthy tissue. Moreover, because the photodynamic effect is confined to a limited illuminated area, PDT is impractical for treating metastases given that whole-body irradiation, including internal regions, would be challenging particularly at requisite light intensities. Indeed, as with all light-related applications, PDT effectiveness is constrained by limited light penetration, even in the NIR, and the local nature of the treatment. Only tumors situated ≤1.5 cm beneath the skin can be effectively damaged [78]. However, more energetic electromagnetic radiation can potentially overcome the seemingly insurmountable obstacle of the penetration depth of light: X ray-activated PDT occurs when X-rays are transduced to UV/Vis light by leveraging wide band gap materials as scintillators. Such materials include metal–organic frameworks, gold nanoclusters, radioluminescent nanophosphors, QDs, and lanthanide-based NPs. The emission of UV/visible light can be subsequently harvested by nearby PSs to generate ROS [66]. This transition from energetic to less energetic photons in deep tissues enables the high depth of penetration enjoyed by radiation in the x-ray regime. X-PDT displays other advantages too, including its ability to remain unconstrained by oxygen levels, and that it can be designed such that substantially reduced radiation levels (<5 Gy) are required for tumor ablation compared to traditional radiation therapy (50~80 Gy) [91]. Ce^{3+}-doped lanthanum(III) fluoride (LaF_3 :Ce^{3+}) NPs and protoporphyrin IX (PPIX) loaded poly(d,l-lactide-co-glycolide (PLGA) microspheres were developed for cancer applications. Here, energy transferred from LaF_3:Ce^{3+} NPs to PPIX upon X-ray irradiation (2 Gy) generated $^1O_2$ to damage cancer cells [92]. In another example, a core–shell Ce^{III}-doped $LiYF_4$@SiO_2@ZnO structure was designed to emit UV light from the Ce^{III}-doped $LiYF_4$ nanoscintillator upon X-ray irradiation [93]. This process enabled the generation of electron–hole (e^-–h^+) pairs in ZnO NPs, leading to the formation of hydroxyl radicals for enhanced antitumor therapeutic efficacy with minimal dependence on the depth and oxygen levels. The mechanism is analogous to a type I PDT process. While the biomedical applications of X-PDT remain in the early development, the field's promise is apparent and poised to generalize the power of PDT to deep tissues.

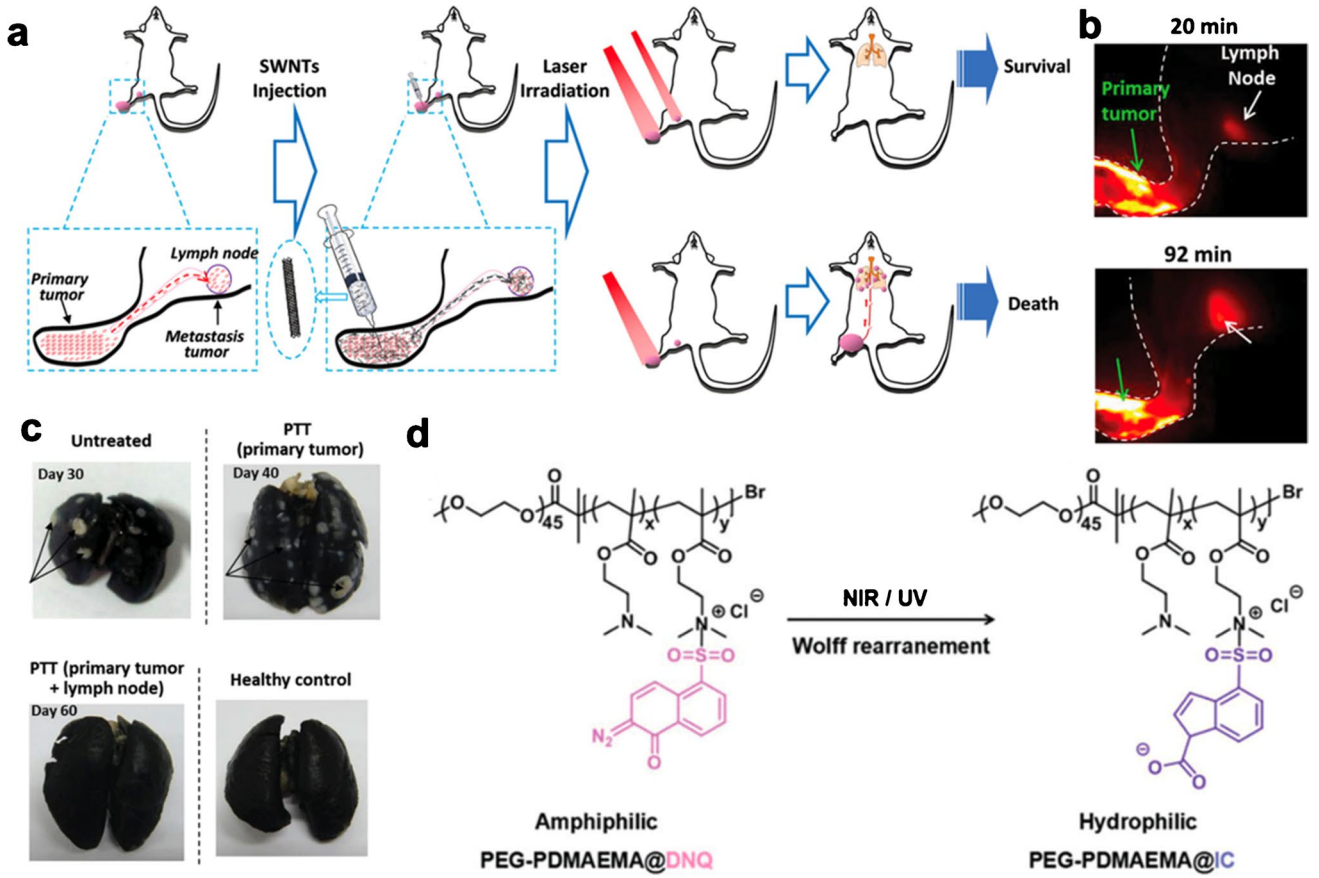


Fig. 9 a) Schematic of single-walled carbon nanotube (SWNT)-PEG being intratumorally injected into the primary 4T1 tumor on the right hind foot. SWNTs were transported into the sentinel lymph node via lymphatic vessels within 20 mins. PTT was then conducted by illuminating both the primary tumor and the lymph node with NIR light [97]. b) NIR-II fluorescent imaging of a tumor-bearing mouse taken at different time points after injection with SWNT–PEG. c) Photos of India ink-stained whole lungs. Copyright 2014 Wiley. d) Chemical structure of PEG-PDMAEMA@ DNQ and its hydrophilic counterpart after Wolff rearrangement under NIR or UV light irradiation. Copyright 2018 The royal society of chemistry

Photothermal

Photothermal therapy (PTT) is a treatment method that utilizes light-absorbing agents (such as gold NPs, iron oxide NPs, graphene NPs, Platinum NPs, dyes) to convert light energy (typically ranging from ~700-1400 nm) into thermal energy. This energy is then selectively applied to target tissues, often cancerous cells, using heat to induce cell death [94, 95]. Unlike PDT, the efficacy of PTT is generally independent of oxygen levels because it relies on heat generation, which in turn can also enhance blood flow within the tumor. Scientists have used mild temperatures (<45 °C) rather than high temperatures to kill cancer cells, as higher temperatures (45–90 °C) may more likely affect both cancer and nearby normal cells (e.g., through enzymatic and mitochondrial dysfunction) and ultimately necrosis [96]. Even if PTT agents such as PEGylated carbon nanotubes are directly injected into the disease site, e.g., intratumorally injected, they may still accumulate in tumor-adjacent lymph nodes [97] (which are not necessarily cancerous) within a short time period (e.g., 20 min, Fig 9a-b). The temperatures of tumor and lymph node increased to ~55 °C and 47 °C upon NIR illumination, respectively, after intratumoral injection of PEGylated single walled carbon nanotubes as a PTT agent. To increase the therapeutic efficiency and decrease tumor metastasis, NIR was illuminated on both tumor and lymph node at two different power densities (0.8 W cm^{-2} for lymph node vs. 0.5 W cm^{-2} for tumor) to compensate for the lower accumulation of carbon nanotubes in the lymph node. This strategy thus remarkably inhibited pulmonary metastasis and offers greatly improved animal survival (Fig 9c).

Upon mild PTT, substantial heat shock protein (Hsp) upregulation typically occurs. Hsps can enhance the heat stress tolerance of cancer cells and increase the likelihood of tumor recurrence [94, 98]. Therefore, Hsp inhibitors (such as small interfering RNA, ATP inhibitor (glucose oxidase), 17-allylamino-17-demethoxygeldanamycin, Gambogic acid) can be delivered to inhibit synthesis of Hsp and thereby

improve PTT therapeutic efficacy [98]. Other parameters such as NP size, morphology, surface modification, as well as NIR power intensity, and wavelength are critical to PTT outcome. For example, gold nanostars show higher photothermal conversion efficiency than gold nanospheres and gold nanorods upon illumination of 808 nm NIR light due to their larger surface area [99]. Small platinum NPs (2 nm) show 5% and 6% higher photothermal efficiency than their 80 nm counterparts at identical total mass upon irradiation of 650 nm and 808 nm laser, respectively [100]. This effect also occurs with other metallic NPs: normalized by total mass, smaller Au NPs display better absorption capacity and higher PTT efficacy because they require much less laser energy than larger Au NPs to kill a tumor cell [101]. Three major NIR parameters, wavelength (~730~840 nm), intensity (1.85~9.75 W/cm^2), and power (105~800 mW), have shown intriguing impact on PTT effects using poly(acrylic acid)-coated superparamagnetic iron oxide NPs [102]. The selection of an appropriate NIR wavelength is often essential for successful in vivo experiments, as water, hemoglobin, lipids, and melanin within the biological environment absorb photons, and biological tissues scatter photons, which significant restricts tissue penetration depth particularly in the visible spectrum (several mm) [103].

In addition to metallic NPs, carbon-based NPs (carbon quantum dots, graphene nanosheets, carbon nanotubes, etc.), semiconductor-based NPs (MoO_{3-x}, WO_{3-x}, etc.), and organic molecules (indocyanine green, polypyrrole polyaniline, etc.) have been used extensively for PTT [95]. However, clinical application of these photothermal NPs may be challenging. The clinical safety profile of AuroLase® therapy, which began initial pre-clinical studies in the 1990s, is based on PEGylated silica-gold nanoshells (Auroshells™) and has only recently been published. It remains under multisite clinical trials [104]. The safety profile for intravenous administration of Auroshells™ was demonstrated in patients with prostate cancer. Yet an important limitation is the heterogeneity in the accumulation of Auroshells™ within a tumor site after intravenous administration due to the heterogeneous tumor vasculature [105]. Pharmacological methods, such as vascular permeabilization, vascular normalization, vascular disruption, could be potentially used to overcome the heterogeneity of Auroshell^{TM} distribution within the tumor in future clinical trials [106].

In addition to the photo-mechanisms applied to therapeutic and imaging applications described in sections "Photoisomerization" to "Photothermal", UV or NIR light can also induce molecular restructuring of light-sensitive chromophores, a phenomenon known as photorearrangement. Photorearrangement is a photochemical reaction wherein a molecule undergoes a structural change that involves a reorganization of its atomic connectivity. The product is a different molecule from the reactant rather than simply an isomer. By contrast, during a photoisomerization process, a molecule changes its geometric or stereochemical structure without altering the atomic connectivity and the product is an isomer of the reactant. A notable example of photorearrangement is the conversion of hydrophobic 2-diazo-1,2-naphthoquinone (DNQ) to the hydrophilic 3-indenecarboxylic acid (ICA) moiety through a light-triggered Wolff rearrangement (Fig 9d) [107]. This transformation from hydrophobic to hydrophilic properties has been used to initiate the breakdown of micelles and organic NPs, thereby releasing encapsulated drugs [108].

Conclusions and perspectives

Leveraging light as an external trigger for therapeutic and diagnostic applications including drug delivery offers advantages such as precise spatiotemporal control, minimal invasiveness, and the ability to sequentially deliver payloads on demand, thus enhancing efficacy and functionality in drug delivery and imaging applications. This systematic review encompasses a wide array of photoactive drug delivery systems employing various mechanisms, including photocleavage, photoisomerization, photopolymerization, photosensitization, photothermal, and photorearrangement. Still, despite promising initial results in this field, substantial challenges remain to be overcome to reach clinical applicability and success.

(1) Photoisomerization is a promising mechanism upon which to develop diverse drug delivery platforms. However, key photoisomer molecules such as some AZO molecules can undergo irreversible degradation upon exposure to light or through enzymatic action by azoreductase, resulting in potential *in vivo* toxicity [39]. Moroever, long photocleavage reaction times do not achieve controlled drug release in a timely manner; for example, ~50 h NIR irradiation was required to release 100% of the drug from photocleavable micelles [43]. Similarly, cleavage of ONB results in the production of highly cytotoxic reactive nitrosobenzaldehyde, which can inhibit enzymatic activity and lead to undesired side effects in vivo [39]. Thus, it will be necessary to evaluate the safety of nanocomposites and photoresponsive molecules and to design around these toxic byproducts. Key safety tests include photostability tests, in vitro/vivo toxicity tests including hemocompatibility of the nanocomposites, and phototoxicity tests to evaluate the toxicity of the light itself independent of the drug.
(2) The short lifetime of $^1O_2$ (< 0.04μs in water environment) limits PDT-induced oxidative damaged to a ~10 nm radius, centered at its production point [73], requir-

ing many such sites to reach efficacy. The efficacy of PDT is also dependent on oxygen levels and oxygen consumption rate. Therefore, strategies to relieve the hypoxic tumor environment are highly likely to substantially improve PDT efficacy [109]. Approaches include design of hemoglobin-encapsulated liposomes, use of reactive oxygen supply materials to react with acid and H_2O_2 for in vivo production of O_2, administration of hypoxia-inducible factor inhibitors, and the development of type I photosensitizers with reduced oxygen consumption [110].

(3) UV light has limited clinical application due to its biological phototoxicity and poor tissue penetration. NIR and visible light are biologically friendly, yet the penetration depth of Vis and NIR I remain limited to ~1 mm and ~10 mm [111, 112], respectively. The NIR-II window offers deeper penetration depth (up to 3 cm) in many tissues [13], motivating research in controlled drug delivery paradigms in deeper tissues (liver, kidney, lung) in rodent models. In addition, optical device-(e.g., optical fibers and capsules) assisted drug delivery systems have been developed to circumvent some light penetration-related limitations. For example, an interstitial NIR light source, percutaneously inserted beneath the tumor with a needle and catheter and using a cylindrical diffusing optical fiber (0.98 mm diameter), was used to treat human epidermoid tumor-bearing mice [107, 113]. However, inserting interstitial light sources into tissues or tumors can be technically challenging and usually requires invasive procedures. This complexity increases the risk of procedural complications and limits the applicability of such approaches, especially in cases where minimally-invasive treatments are preferred. Thus, development of less-invasive delivery systems with higher tissue penetration depths is needed [12].

(4) Most photo-controlled drug delivery systems are irreversible, which can restrict the ability to finely and precisely control the timing and dosage of drug release, potentially leading to suboptimal therapeutic outcomes or unwanted side effects [11]. Thus, developing reversible, light-controlled drug delivery systems, including by incorporating photoswitchable molecules such as SPs and AZOs that use cytocompatible wavelengths and power, is crucial to fine-tune photonic-related therapeutic effects in vivo.

(5) The US FDA has thus far approved over ten drug nanocarriers for clinical use, including Doxil (Liposomal/DOX), Abraxane (Nanoparticulate albumin/paclitaxel), and ThermoDox (Temperature-sensitive DOX liposome) [107]. However, photoactivated drug delivery systems have not yet been approved for use in clinical settings, and the process of gaining clinical approval can be very time-consuming. For instance, pre-clinical studies of AuroLase® therapy, employing PEGylated gold nanoshells, commenced in the 1990s and remain in ongoing multi-site clinical trials [104]. Moreover, addressing long-term biosafety concerns and achieving scaled-up production of nanocarriers represent significant technical challenges for clinical applications. Furthermore, sufficiently extensive evaluation of the byproducts generated from phototriggered cascade reactions is still pending.

(6) Polymers are widely used in drug delivery systems (DDS) due to their advantageous properties, including ease of fabrication and design, diverse structural options, good biocompatibility, and potential to select for degradable options [114]. There currently exist a number of FDA-approved polymer-based DDS available on the market, such as Neulasta and Copaxone. Neulasta is a recombinant PEGylated human granulocyte colony-stimulating factor used for chemotherapy-induced neutropenia in patients [115]. Copaxone, a formulation of polypeptide co-polymers, has been used for Multiple Sclerosis [116]. However, the range of polymeric materials currently suitable for use as DDS remains limited. Future developments in polymeric DDS will need to address challenges such as limited selectivity and restricted tissue penetration [117]. Additionally, alternative strategies such as combining polymers with biologics or utilizing nanotechnology to create hybrid systems may offer even more targeted and efficient drug delivery solutions, improving the chances of clinical efficacy in the future.

(7) While light irradiation can be performed specifically at the disease site to avoid undesirable toxicity to normal tissues, real-time tracking of the distribution and amount of drug release in the living body, such as through image-guided photoresponsive drug delivery and drug release monitoring, should be developed. Such technology will be important to monitor the progress of treatment to ensure sufficient levels of drug are reaching the disease site to achieve optimal therapeutic efficacy.

In summary, there remains significant potential for innovative research on light-responsive NPs for biomedical applications. This rapidly advancing field is poised to generate breakthroughs for disease diagnosis and treatment, primarily for superficial and endoscopically- or surgically accessible applications in clinical medicine.

Author contribution YZ and BRS conceived the manuscript. YZ wrote and revised the manuscript, YQ and ABK revised the manuscript, BRS supervised and edited the manuscript. All authors read and approved the final manuscript.

Funding This work was financially supported by NIH grant R01 CA244491 from the NCI, pilot grants from the Henry Ford-Michigan State alliance, an American Cancer Society Research Scholar grant (RSG-23–1156695-01-ET) (to BRS), and a Perkin-Elmer post-doctoral fellowship (to YZ).

Data availability The present study did not include generation of data nor specific data analyses, so data availability is not applicable.

Declarations

Ethics approval Not required since no human participants or animals were recruited for this study.

Conflict of interest The authors declare no competing interests.

Database and search strategy We used Google Scholar as the primary database and information source. We searched the recently published literature (within 15 years) with the following keywords individually and in relevant combinations: light responsive, nanoparticle, drug release, mechanism, photothermal, photosensitization, photopolymerization, photocleavage, and photoisomerization.

References

1. Mohanraj VJ, Chen Y. Nanoparticles - A review. Trop J Pharm Res. 2007;5:561–73.
2. Liu Y, Yang G, Jin S, Xu L, Zhao CX. Development of High-Drug-Loading Nanoparticles. Chempluschem. 2020;85:2143–57.
3. Directions F. Controlled Drug Delivery Systems: Current Status and future directions. Molecules. 2021;26:5905.
4. Kamaly N, Yameen B, Wu J, Farokhzad OC. Degradable controlled-release polymers and polymeric nanoparticles: Mechanisms of controlling drug release. Chem Rev. 2016;116:2602–63.
5. Xu C, et al. A pH-responsive charge-reversal drug delivery system with tumor-specific drug release and ROS generation for cancer therapy. Int J Nanomedicine. 2020;15:65–80.
6. Guo X, et al. Advances in redox-responsive drug delivery systems of tumor microenvironment. J Nanobiotechnology. 2018;16:1–10.
7. Shahriari M, et al. Enzyme responsive drug delivery systems in cancer treatment. J Control Release. 2019;308:172–89.
8. Song XR, et al. Enhancing Antitumor Efficacy by Simultaneous ATP-Responsive Chemodrug Release and Cancer Cell Sensitization Based on a Smart Nanoagent. Adv Sci. 2018;5(12):1801201.
9. Akimoto J, Nakayama M, Okano T. Temperature-responsive polymeric micelles for optimizing drug targeting to solid tumors. J Control Release. 2014;193:2–8.
10. Wang H, Yi J, Mukherjee S, Banerjee P, Zhou S. Magnetic/NIR-thermally responsive hybrid nanogels for optical temperature sensing, tumor cell imaging and triggered drug release. Nanoscale. 2014;6:13001–11.
11. Abdelmohsen HAM, Copeland NA, Hardy JG. Light-responsive biomaterials for ocular drug delivery. Drug Deliv Transl Res. 2023;13:2159–82.
12. Zhao W, et al. Remote Light-Responsive Nanocarriers for Controlled Drug Delivery: Advances and Perspectives. Small. 2019;15:1–34.
13. Mu J, et al. The Chemistry of Organic Contrast Agents in the NIR-II Window. Angew Chemie - Int Ed. 2022;61:e202114722.
14. Raza A, Hayat U, Rasheed T, Bilal M, Iqbal HMN. 'Smart' materials-based near-infrared light-responsive drug delivery systems for cancer treatment: A review. J Mater Res Technol. 2019;8:1497–509.
15. Olejniczak J, Carling CJ, Almutairi A. Photocontrolled release using one-photon absorption of visible or NIR light. J Control Release. 2015;219:18–30.
16. Dudek M, et al. Two-photon absorption and two-photon-induced isomerization of azobenzene compounds. RSC Adv. 2020;10:40489–507.
17. Wu S, Butt HJ. Near-Infrared-Sensitive Materials Based on Upconverting Nanoparticles. Adv Mater. 2016;28:1208–26.
18. Ansari AA, Sillanpää M. Advancement in upconversion nanoparticles based NIR-driven photocatalysts. Renew Sustain Energy Rev. 2021;151:111631.
19. Kress J, et al. A dual-channel endoscope for quantitative imaging, monitoring, and triggering of doxorubicin release from liposomes in living mice. Sci Rep. 2017;7:1–13.
20. Saneja A, et al. Recent advances in near-infrared light-responsive nanocarriers for cancer therapy. Drug Discov Today. 2018;23:1115–25.
21. Pan P, et al. Photosensitive drug delivery systems for cancer therapy: Mechanisms and applications. J Control Release. 2021;338:446–61.
22. Schimka S, et al. Photo-isomerization of azobenzene containing surfactants induced by near-infrared light using upconversion nanoparticles as mediator. J Phys Condens Matter. 2019;31:125201.
23. Bonacchi S, et al. Photoswitchable NIR-Emitting Gold Nanoparticles. Angew Chemie - Int Ed. 2016;55:11064–8.
24. Das G, et al. Azobenzene-Equipped Covalent Organic Framework: Light-Operated Reservoir. J Am Chem Soc. 2019;141:19078–87.
25. Shiraishi Y, et al. Light-Triggered Self-Assembly of Gold Nanoparticles Based on Photoisomerization of Spirothiopyran. Angew Chemie. 2013;125:8462–6.
26. Aznar E, et al. Photochemical and chemical two-channel control of functional nanogated hybrid architectures. Adv Mater. 2007;19:2228–31.
27. Shen H, Zhou M, Zhang Q, Keller A, Shen Y. Zwitterionic light-responsive polymeric micelles for controlled drug delivery. Colloid Polym Sci. 2015;293:1685–94.
28. Cui ZK, et al. Nonphospholipid fluid liposomes with switchable photocontrolled release. Langmuir. 2014;30:10818–25.
29. Levine DH, et al. Polymersomes: A new multi-functional tool for cancer diagnosis and therapy. Methods. 2008;46:25–32.
30. Wang X, et al. Reversibly Switching Bilayer Permeability and Release Modules of Photochromic Polymersomes Stabilized by Cooperative Noncovalent Interactions. J Am Chem Soc. 2015;137:15262–75.
31. Chen S, et al. Nanocomposites of Spiropyran-Functionalized Polymers and Upconversion Nanoparticles for Controlled Release Stimulated by Near-Infrared Light and pH. Macromolecules. 2016;49:7490–6.
32. Liu J, Bu W, Pan L, Shi J. NIR-Triggered Anticancer Drug Delivery by Upconverting Nanoparticles with Integrated Azobenzene-Modified Mesoporous Silica. Angew Chemie. 2013;125:4471–5.
33. Kim B, et al. Reversible Photochemical Switching via Plasmonically Enhanced Upconversion Photoluminescence. Adv Opt Mater. 2021;9:1–11.
34. Jerca FA, Jerca VV, Hoogenboom R. Advances and opportunities in the exciting world of azobenzenes. Nat Rev Chem. 2022;6:51–69.
35. Oliveira H, et al. Critical Considerations on the Clinical Translation of Upconversion Nanoparticles (UCNPs): Recommendations from the European Upconversion Network (COST Action CM1403). Adv Healthc Mater. 2019;8:1801233.

36. Huang Y, et al. A NIR-Triggered gatekeeper of supramolecular conjugated unimicelles with two-photon absorption for controlled drug release. Chem Commun. 2019;55:6735–8.
37. Rojas-Gutierrez PA, et al. A Route to Triggered Delivery via Photocontrol of Lipid Bilayer Properties Using Lanthanide Upconversion Nanoparticles. ACS Appl Nano Mater. 2018;1:5345–54.
38. Zhao T, et al. Near-Infrared Triggered Decomposition of Nanocapsules with High Tumor Accumulation and Stimuli Responsive Fast Elimination. Angew Chemie - Int Ed. 2018;57:2611–5.
39. Tao Y, Chan HF, Shi B, Li M, Leong KW. Light: A Magical Tool for Controlled Drug Delivery. Adv Funct Mater. 2020;30:1–28.
40. Liu Q, et al. A photocleavable low molecular weight hydrogel for light-triggered drug delivery. Chinese Chem Lett. 2019;30:485–8.
41. Liu G, Liu W, Dong CM. UV- and NIR-responsive polymeric nanomedicines for on-demand drug delivery. Polym Chem. 2013;4:3431–43.
42. Zhu H, et al. Folate-modified chitosan micelles with enhanced tumor targeting evaluated by near infrared imaging system. Carbohydr Polym. 2011;86:1118–29.
43. Cao J, et al. Near-infrared light-triggered micelles for fast controlled drug release in deep tissue. Biomaterials. 2013;34:6272–83.
44. Xiang J, et al. Nanocomplexes of Photolabile Polyelectrolyte and Upconversion Nanoparticles for Near-Infrared Light-Triggered Payload Release. ACS Appl Mater Interfaces. 2018;10:20790–800.
45. Wang X, et al. Photo- and pH-responsive drug delivery nanocomposite based on o-nitrobenzyl functionalized upconversion nanoparticles. Polymer. 2021;229:123961.
46. Agasti SS, et al. Photoregulated release of caged anticancer drugs from gold nanoparticles. J Am Chem Soc. 2009;131:5728–9.
47. Shen W, Zheng J, Zhou Z, Zhang D. Approaches for the synthesis of o-nitrobenzyl and coumarin linkers for use in photocleavable biomaterials and bioconjugates and their biomedical applications. Acta Biomater. 2020;115:75–91.
48. Kumar S, et al. Near-infrared light sensitive polypeptide block copolymer micelles for drug delivery. J Mater Chem. 2012;22:7252–7.
49. Arjmand F, Salami-Kalajahi M, Roghani-Mamaqani H. Preparation of photolabile nanoparticles by coumarin-based crosslinker for drug delivery under light irradiation. J Phys Chem Solids. 2021;154:110102.
50. Zeleňák V, et al. Photo-switchable nanoporous silica supports for controlled drug delivery. New J Chem. 2018;42:13263–71.
51. Zhao Y. Light-responsive block copolymer micelles. Macromolecules. 2012;45:3647–57.
52. Cho HJ, Chung M, Shim MS. Engineered photo-responsive materials for near-infrared-triggered drug delivery. J Ind Eng Chem. 2015;31:15–25.
53. Cazin I, Rossegger E, Guedes de la Cruz G, Griesser T, Schlögl S. Recent advances in functional polymers containing coumarin chromophores. Polymers (Basel). 2021;13:1–51.
54. Li Q, Yuan S, Liu F, Zhu X, Liu J. Lanthanide-Doped Nanoparticles for Near-Infrared Light Activation of Photopolymerization: Fundamentals. Optimization and Applications Chem Rec. 2021;21:1681–96.
55. Sadasivuni, K. K. et al. 2019 Lecture Notes in Bioengineering: Polymer Nanocomposites in Biomedical Engineering. Progress in Polymer Science vol. 80
56. Cui L, et al. Reduction Triggered in Situ Polymerization in Living Mice. J Am Chem Soc. 2020;142:15575–84.
57. Tyagi P, Barros M, Stansbury JW, Kompella UB. Light-activated, in situ forming gel for sustained suprachoroidal delivery of bevacizumab. Mol Pharm. 2013;10:2858–67.
58. Cinay GE, et al. Nanogel-Integrated pH-Responsive Composite Hydrogels for Controlled Drug Delivery. ACS Biomater Sci Eng. 2017;3:370–80.
59. Nasr FH, Khoee S, Dehghan MM, Chaleshtori SS, Shafiee A. Preparation and Evaluation of Contact Lenses Embedded with Polycaprolactone-Based Nanoparticles for Ocular Drug Delivery. Biomacromol. 2016;17:485–95.
60. Roh YH, et al. Photocrosslinked DNA nanospheres for drug deliverya. Macromol Rapid Commun. 2010;31:1207–11.
61. Zhang L, et al. Dual Role of Doxorubicin for Photopolymerization and Therapy. Biomacromol. 2020;21:3887–97.
62. Yu S, et al. Preparation of PMMA-Based Temperature/pH Responsive Nanoparticles Encapsulating 5-Fluorouracil and Methotrexate In Situ by One-Pot Dispersion Photopolymerization. Macromol Biosci. 2024;24(5):2300469.
63. Beyazit S, et al. Versatile synthetic strategy for coating upconverting nanoparticles with polymer shells through localized photopolymerization by using the particles as internal light sources. Angew Chemie - Int Ed. 2014;53:8919–23.
64. Darani MK, Bastani S, Ghahari M, Kardar P, Mohajerani E. NIR induced photopolymerization of acrylate-based composite containing upconversion particles as an internal miniaturized UV sources. Prog Org Coatings. 2017;104:97–103.
65. Ruan Z, et al. High Singlet Oxygen Yield Photosensitizer Based Polypeptide Nanoparticles for Low-Power Near-Infrared Light Imaging-Guided Photodynamic Therapy. Bioconjug Chem. 2018;29:3441–51.
66. Zhou Z, Song J, Nie L, Chen X. Reactive oxygen species generating systems meeting challenges of photodynamic cancer therapy. Chem Soc Rev. 2016;45:6597–626.
67. Rajendran M. Quinones as photosensitizer for photodynamic therapy: ROS generation, mechanism and detection methods. Photodiagnosis Photodyn Ther. 2016;13:175–87.
68. Zhuang J, et al. Efficient NIR-II Type-I AIE Photosensitizer for Mitochondria-Targeted Photodynamic Therapy through Synergistic Apoptosis-Ferroptosis. ACS Nano. 2023;17:9110–25.
69. Lushchak VI. Free radicals, reactive oxygen species, oxidative stress and its classification. Chem Biol Interact. 2014;224:164–75.
70. Li Y, et al. A Cascade Strategy Boosting Hydroxyl Radical Generation with Aggregation-Induced Emission Photosensitizers-Albumin Complex for Photodynamic Therapy. ACS Nano. 2023;17:16993–7003.
71. Correia JH, Rodrigues JA, Pimenta S, Dong T, Yang Z. Photodynamic therapy review: Principles, photosensitizers, applications, and future directions. Pharmaceutics. 2021;13:1–16.
72. Sheng T, Ong Y, Busch TM, Zhu TC. Reactive oxygen species explicit dosimetry to predict local tumor growth for Photofrin-mediated photodynamic therapy. Biomed Opt Express. 2020;11:4586.
73. Sai DL, Lee J, Nguyen DL, Kim YP. Tailoring photosensitive ROS for advanced photodynamic therapy. Exp Mol Med. 2021;53:495–504.
74. Liu WL, et al. Aggressive Man-Made Red Blood Cells for Hypoxia-Resistant Photodynamic Therapy. Adv Mater. 2018;30:1–10.
75. Sitnik TM, Hampton JA, Henderson BW. Reduction of tumour oxygenation during and after photodynamic therapy in vivo: Effects of fluence rate. Br J Cancer. 1998;77:1386–94.
76. Kawauchi S, et al. Differences between cytotoxicity in photodynamic therapy using a pulsed laser and a continuous wave laser: Study of oxygen consumption and photobleaching. Lasers Med Sci. 2004;18:179–83.
77. Karges J. Clinical Development of Metal Complexes as Photosensitizers for Photodynamic Therapy of Cancer. Angew Chemie - Int Ed. 2022;61:e202112236.

78. Lan M, et al. Photosensitizers for Photodynamic Therapy. Adv Healthc Mater. 2019;8:1–37.
79. Lo PC, et al. The unique features and promises of phthalocyanines as advanced photosensitisers for photodynamic therapy of cancer. Chem Soc Rev. 2020;49:1041–56.
80. Brilkina AA, et al. Photobiological properties of phthalocyanine photosensitizers Photosens, Holosens and Phthalosens: A comparative in vitro analysis. J Photochem Photobiol B Biol. 2019;191:128–34.
81. Lange N, Szlasa W, Saczko J, Chwiłkowska A. Potential of cyanine derived dyes in photodynamic therapy. Pharmaceutics. 2021;13:1–17.
82. Heinemann F, Karges J, Gasser G. Critical Overview of the Use of Ru(II) Polypyridyl Complexes as Photosensitizers in One-Photon and Two-Photon Photodynamic Therapy. Acc Chem Res. 2017;50:2727–36.
83. Wang L. Recent Advances in Metal-Based Molecular Photosensitizers for Artificial Photosynthesis. Catalysts. 2022;12:919.
84. Zhang L, Ding D. Recent advances of transition Ir(III) complexes as photosensitizers for improved photodynamic therapy. View. 2021;2:1–14.
85. Li SPY, Liu HW, Zhang KY, Lo KKW. Modification of luminescent iridium(III) polypyridine complexes with discrete polyethylene glycol (PEG) pendants: Synthesis, emissive behavior, intracellular uptake, and PEGylation properties. Chem - A Eur J. 2010;16:8329–39.
86. Lan G, et al. Nanoscale Metal-Organic Layers for Deeply Penetrating X-ray-Induced Photodynamic Therapy. Angew Chemie. 2017;129:12270–4.
87. Kuang S, et al. A Mitochondrion-Localized Two-Photon Photosensitizer Generating Carbon Radicals Against Hypoxic Tumors. Angew Chemie - Int Ed. 2020;59:20697–703.
88. Kassab G, et al. Structural Effect of Rhenium- and Iridium-Complex Liposome Composition on Their Selectivity for Antimicrobial Photodynamic Therapy. Small Sci. 2024;4(2):2300131.
89. Li J, Chen T. Transition metal complexes as photosensitizers for integrated cancer theranostic applications. Coord Chem Rev. 2020;418:213355.
90. Tang Y, et al. Oxygen-independent organic photosensitizer with ultralow-power NIR photoexcitation for tumor-specific photodynamic therapy. Nat Commun. 2024;15:1–13.
91. Sun W, Zhou Z, Pratx G, Chen X, Chen H. Nanoscintillator-mediated X-ray induced photodynamic therapy for deep-seated tumors: From concept to biomedical applications. Theranostics. 2020;10:1296–318.
92. Zou X, et al. X-ray-induced nanoparticle-based photodynamic therapy of cancer. Nanomedicine. 2014;9:2339–51.
93. Zhang C, et al. Marriage of scintillator and semiconductor for synchronous radiotherapy and deep photodynamic therapy with diminished oxygen dependence. Angew Chemie - Int Ed. 2015;54:1770–4.
94. Kadkhoda J, Tarighatnia A, Barar J, Aghanejad A, Davaran S. Recent advances and trends in nanoparticles based photothermal and photodynamic therapy. Photodiagnosis Photodyn Ther. 2022;37:102697.
95. Zhao L, et al. Recent advances in selective photothermal therapy of tumor. J Nanobiotechnology. 2021;19:1–15.
96. Akbarian A, et al. Association between heat stress and oxidative stress in poultry; mitochondrial dysfunction and dietary interventions with phytochemicals. J Anim Sci Biotechnol. 2016;7:1–4.
97. Liang C, et al. Tumor metastasis inhibition by imaging-guided photothermal therapy with single-walled carbon nanotubes. Adv Mater. 2014;26:5646–52.
98. Zhang G, Cheng W, Du L, Xu C, Li J. Synergy of hypoxia relief and heat shock protein inhibition for phototherapy enhancement. J Nanobiotechnology. 2021;19:1–13.
99. Yang W, et al. Shape effects of gold nanoparticles in photothermal cancer therapy. Mater Today Sustain. 2021;13:100078.
100. Depciuch J, et al. Size effect of platinum nanoparticles in simulated anticancer photothermal therapy. Photodiagnosis Photodyn Ther. 2020;29:1–7.
101. Yang W, Liang H, Ma S, Wang D, Huang J. Gold nanoparticle based photothermal therapy: Development and application for effective cancer treatment. Sustain Mater Technol. 2019;22:e00109.
102. Bilici K, Muti A, Demir Duman F, Sennaroğlu A, Yağci Acar H. Investigation of the factors affecting the photothermal therapy potential of small iron oxide nanoparticles over the 730–840 nm spectral region. Photochem Photobiol Sci. 2018;17:1787–93.
103. Liu Y, et al. Versatile Types of Inorganic/Organic NIR-IIa/IIb Fluorophores: From Strategic Design toward Molecular Imaging and Theranostics. Chem Rev. 2022;122:209–68.
104. D Melo-Diogo de C Pais-Silva DR Dias AF Moreira IJ Correia 2017 Strategies to Improve Cancer Photothermal Therapy Mediated by Nanomaterials Adv. Healthc Mater 6
105. Movia D, Benhaddada M, Spadavecchia J, Prina-Mello A. Latest Advances in Combining Gold Nanomaterials With Physical Stimuli Towards New Responsive Therapeutic and Diagnostic Strategies. Precis Nanomedicine. 2020;3:495–524.
106. Izci M, Maksoudian C, Manshian BB, Soenen SJ. The Use of Alternative Strategies for Enhanced Nanoparticle Delivery to Solid Tumors. Chem Rev. 2021;121:1746–803.
107. Xiong Q, et al. Photoactive Nanocarriers for Controlled Delivery. Adv Funct Mater. 2020;30:1–17.
108. Li Q, Cao Z, Wang G. Diazonaphthoquinone-based amphiphilic polymer assemblies for NIR/UV light- and pH-responsive controlled release. Polym Chem. 2018;9:463–71.
109. Shen Z, et al. Strategies to improve photodynamic therapy efficacy by relieving the tumor hypoxia environment. NPG Asia Mater. 2021;13:1–19.
110. Lu B, Wang L, Tang H, Cao D. Recent advances in type I organic photosensitizers for efficient photodynamic therapy for overcoming tumor hypoxia. J Mater Chem B. 2023;11:4600–18.
111. Chen Y, Xue L, Zhu Q, Feng Y, Wu M. Recent Advances in Second Near-Infrared Region (NIR-II) Fluorophores and Biomedical Applications. Front Chem. 2021;9:1–12.
112. Teraphongphom N, Kong CS, Warram JM, Rosenthal EL. Specimen mapping in head and neck cancer using fluorescence imaging. Laryngoscope Investig Otolaryngol. 2017;2:447–52.
113. Maruoka Y, et al. Near Infrared Photoimmunotherapy with Combined Exposure of External and Interstitial Light Sources. Mol Pharm. 2018;15:3634–41.
114. El-Say KM, El-Sawy HS. Polymeric nanoparticles: Promising platform for drug delivery. Int J Pharm. 2017;528:675–91.
115. Elsadek NE, et al. Pegfilgrastim (PEG-G-CSF) induces anti-PEG IgM in a dose dependent manner and causes the accelerated blood clearance (ABC) phenomenon upon repeated administration in mice. Eur J Pharm Biopharm. 2020;152:56–62.
116. Jalilian B, Einarsson HB, Vorup-Jensen T. Glatiramer acetate in treatment of multiple sclerosis: A toolbox of random co-polymers for targeting inflammatory mechanisms of both the innate and adaptive immune system? Int J Mol Sci. 2012;13:14579–605.
117. Indoria S, Singh V, Hsieh MF. Recent advances in theranostic polymeric nanoparticles for cancer treatment: A review. Int J Pharm. 2020;582:119314.

Publisher's Note Springer Nature remains neutral with regard to jurisdictional claims in published maps and institutional affiliations.

Springer Nature or its licensor (e.g. a society or other partner) holds exclusive rights to this article under a publishing agreement with the author(s) or other rightsholder(s); author self-archiving of the accepted manuscript version of this article is solely governed by the terms of such publishing agreement and applicable law.